Generation of entangled photons via parametric down-conversion in semiconductor lasers and integrated quantum photonic systems

Mikhail Tokman,[1] Yongrui Wang,[2] Qianfan Chen,[2] Leon Shterengas,[3] and Alexey Belyanin[2]
[1]*Institute of Applied Physics, Russian Academy of Sciences, Nizhny Novgorod 603950, Russia*
[2]*Department of Physics and Astronomy, Texas A&M University, College Station, Texas 77843, USA*
[3]*State University of New York at Stony Brook, Stony Brook, New York 11794, USA*

(Received 29 October 2021; revised 6 February 2022; accepted 23 February 2022; published 14 March 2022)

We propose and design a high-brightness, ultracompact electrically pumped GaSb-based laser source of entangled photons generated by mode-matched intracavity parametric down-conversion of lasing modes. To describe the nonlinear mixing in highly dispersive and dissipative waveguides, we develop a nonperturbative quantum theory of parametric down-conversion of waveguide modes which takes into account the effects of modal dispersion, group and phase mismatch, propagation, dissipation, and coupling to noisy reservoirs. We extend our theory to the regime of quantized pump fields with an approach based on the propagation equation for the state vector which solves the nonperturbative boundary-value problem of the parametric decay of a quantized single-photon pump mode and can be generalized to include the effects of dissipation and noise. Our formalism is applicable to a wide variety of three-wave mixing propagation problems. It provides convenient analytic expressions for interpreting experimental results and predicting the performance of monolithic quantum photonic systems.

DOI: 10.1103/PhysRevA.105.033707

I. INTRODUCTION

Spontaneous parametric down-conversion (SPDC) has become a benchmark process for generation of entangled photon pairs and heralded single photons in a variety of experiments and for the needs of the rapidly growing field of quantum information processing; see, e.g., [1,2] for recent reviews. Typically, the second-order nonlinear susceptibility $\chi^{(2)}$ of birefringent crystals cut at an angle to satisfy the phase-matching condition for a specific SPDC process is used; see for instance [3]. The utilization of periodically poled nonlinear crystals making use of quasi-phase matching led to improved performance. Recent advances in high-quality microcavities, nanoantennas, and metamaterials have led to the prediction [4–6] and realization (e.g., [7–10]) of compact chip-scale parametric down-conversion sources. An external optical pump is still required in all cases. Strong second-order nonlinearity of III-V semiconductors in combination with their superior light emission properties can be used for both generation of pump light and production of entangled photon states where waveguides and other photonic integrated circuit components can be utilized to facilitate phase matching and to perform quantum information processing operations [11]. The monolithic integration of the pump laser and SPDC source on the same platform still remains a holy grail of this technology as its availability will dramatically simplify the experimental arrangements and pave the way to the long-sought scalable approach to quantum sensing, quantum communications, and optical quantum computing. It is natural to consider the III-V heterostructures, which can produce high power and stable pump lasers and also demonstrate strong second-order nonlinearities required for SPDC as a potential platform for such integration.

In a standard single core laser waveguide heterostructure the phase-matching conditions for the efficient SPDC process are virtually impossible to achieve because of normal dispersion: the refractive index of all materials away from resonance transitions decreases with wavelength. One recent approach to defeat the normal dispersion limitation was successfully realized in Bragg-reflection waveguides (BRWs) [12], which confine the pump Bragg mode and total internal reflection guided signal and idler modes. The optically pumped BRW devices have been extensively studied [12–14]. An intracavity nondegenerate optical parametric generation in an electrically injected GaAs-based BRW laser was demonstrated in [15] and corresponding emitters of correlated photons generating broadband product states of the near-infrared signal and idler photons were reported [16]. However, the design complications associated with the presence of Bragg reflectors comprising the device claddings so far led to strong degradation of the near-infrared pump laser performance parameters. It is also not trivial to arrange for stable single mode operation of the BRW pump laser for the same reason. These issues were recognized even for near-infrared BRW emitters where the vertical cavity surface emitting laser technology development led to significant advances in design of the Bragg reflector claddings. In GaSb-based lasers capable of intracavity SPDC generation of midinfrared (MWIR) correlated photon pairs the situation with BRWs is much less developed and it would be extremely challenging to arrange for efficient carrier transport through thick Bragg reflectors comprising the cladding layers of these devices.

We propose a different approach to achieve phase matching between $\approx$2-μm pump and $\approx$4-μm signal and idler waves which is compatible with GaSb-based and any other semiconductor laser technology. It relies on the natural TE polarized

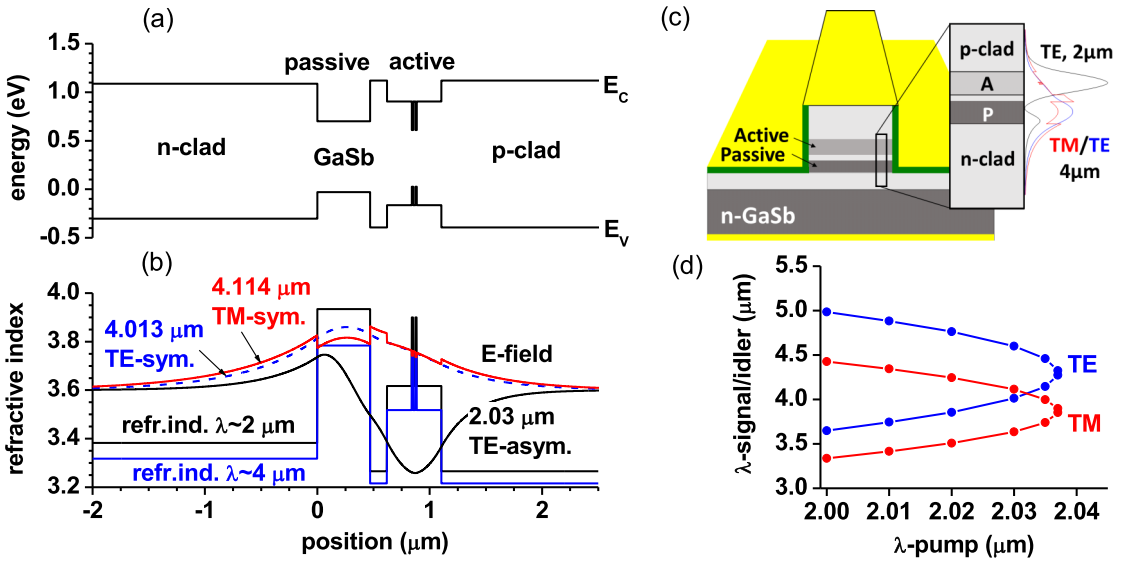

FIG. 1. (a) Band diagram of the GaSb-based coupled-waveguide laser heterostructure and (b) refractive index and electric-field profiles for the TE polarized $\lambda = 2.03$ μm asymmetric pump mode (black solid line), TE polarized $\lambda = 4.013$ μm fundamental signal mode (blue dashed line), and TM polarized $\lambda = 4.114$ μm fundamental idler mode (red solid line). The passive waveguide width is 470 nm and the separation barrier between two waveguide cores is 150 nm. The position is along the growth direction. (c) Sketch of a generic laser device with a coupled waveguide for mode-matched type-II intracavity SPDC of laser photons. The profiles of mode intensities [same as in (b)] are superimposed on the inset. (d) Calculated wavelengths of the signal and idler modes at exact phase matching as a function of the pump mode wavelength.

pump mode and utilizes type-II SPDC to produce biphotons and polarization entangled photon pairs as required for quantum technologies. Both degenerate and nondegenerate type-II SPDC are possible and, moreover, can be easily selected by tuning the pump wavelength using standard techniques. Our proposed GaSb-based laser heterostructure illustrated in Fig. 1 has a coupled-waveguide design favoring lasing near ≈ 2 μm (pump) in TE polarized asymmetric supermode. The type-II SPDC process will produce entangled photon pairs in TE and TM polarized symmetric supermodes. The use of the asymmetric supermode allows us to reduce the effective refractive index of the $\approx$2-μm pump to achieve efficient phase matching with $\approx$4-μm signal and idler symmetric supermodes. The device geometry makes maximum use of the large $|\chi^{(2)}_{xyz}| >$ 200 pm/V of III-V zinc-blende semiconductors for the SPDC process, which is significantly higher as compared to conventional nonlinear crystals [17].

The theory of entangled photon state generation in semiconductor lasers and waveguides has important peculiarities and challenges which have not been addressed before. First, laser waveguides and other monolithic integrated photonic systems are inherently highly dispersive and dissipative. Including the effects of dispersion, dissipation, and noise in a consistent way is crucial for predicting the performance of these devices. For example, we show below that the quantum noise can make a significant and even dominant contribution within the signal and idler bandwidth even at low ambient temperature.

Second, while SPDC and a closely related process of squeezed vacuum generation have been typically treated as an initial-value problem for quantized signal and idler fields or a problem of entanglement of quantized cavity modes coupled with free space modes [18–20], the SPDC in a finite-length waveguide presents a boundary-value eigenmode propagation problem affected by phase and group velocity mismatch, dispersion, absorption, and noisy reservoirs.

Third, extra challenges arise in the case of a quantized pump field, e.g., a single-photon pump, as the operator-valued Heisenberg-Langevin equations become nonlinear. While the case of all three quantum fields has been well studied as a mean-field initial-value problem and in the perturbative regime, here we present an approach based on the propagation equation for the state vector which allows us to describe the SPDC process with nonperturbative coupling between quantized single-photon pump, signal, and idler fields as a boundary-value propagation problem. Note that the approaches close to the one presented in this paper were developed in [21–24] for the propagation problem of entangled state generation via four-wave mixing. However, those approaches were not applied to the SPDC process.

The quantum theory of SPDC in monolithic nonlinear waveguides is applicable to any nonlinear propagation problem involving three-wave mixing. It provides convenient analytic expressions for interpreting experimental results. The proposed device design principles can be applied to a wide variety of III-V semiconductor diode lasers. The specific implementation of the monolithic electrically pumped quantum light source within the III-V-Sb platform offers an extra bonus of covering the MWIR spectral region, which holds strong promise for applications in quantum communications, quantum sensing, and imaging. Free space quantum-secured communication links operating in the MWIR range offer significant advantages over near-infrared channels due to lower scattering losses. Satellite-based quantum key distribution

systems [25] based on near-infrared sources are severely constrained by solar background radiation and, until the introduction of $\lambda \sim 1.5$ μm quantum light emitters, were restricted to at night operation [26]. Systems operating near 4 μm will benefit from dramatically reduced solar background and still moderate Earth thermal background [27,28]. Operation at these wavelengths generally improves reliability and throughput of free space quantum-secured links under adverse weather conditions, scattering, and atmospheric turbulence. Recently, quantum illumination protocols relying on correlations between photons in entangled pairs have been experimentally demonstrated to offer more than an order of magnitude image contrast improvement in the presence of background light, sensor noise, and loss [29].

Modern technology for emitting and detecting MWIR entangled photon pairs is based on multiwave mixing in free-standing nonlinear optical elements [30–32]. This puts many exciting applications out of reach. The full integration of the components of photonic quantum information technology is not yet available even for the much more user friendly near-infrared region of the spectrum. The development of quantum information technology in the MWIR region of the spectrum is even less advanced. For MWIR both generation of the entangled photon pairs and single-photon detection require nonlinear converters since even direct single-photon counting photodetectors operating in midinfrared are yet to be developed and realized. The III-V-Sb material system can host electrically injected entangled photon pair emitters together with all other quantum information processing photonic integrated circuit components, thus serving as a common platform for the advancement of MWIR quantum information technology.

II. DIODE LASER DESIGN FOR INTRACAVITY TYPE-II SPDC OF LASER MODES

One example of the laser device design for the intracavity type-II SPDC process is shown in Fig. 1. The laser is grown in the usual ⟨001⟩ direction and has a ridge cavity aligned along the ⟨110⟩ direction; therefore, only the TE ⟶ TE+TM SPDC decay is allowed by zinc-blende crystal symmetry. An example of TM and TE signal and idler modes shown in Fig. 1 corresponds to nondegenerate SPDC in which they have different frequencies and refractive indices. Changing the pump wavelength within the range of ≈10 nm will tune the type-II SPDC from the nondegenerate to degenerate case. Figure 1(d) plots the wavelengths of the phase-matched signal and idler TM and TE polarized photons in symmetric supermodes versus wavelength of the TE polarized pump in asymmetric supermode calculated for the coupled waveguide in Fig. 1(b).

The tuning curves in Fig. 1 correspond to perfect phase-matching conditions. The phase-matching lines are significantly broadened and the SPDC proceeds within a broad bandwidth; see a detailed discussion below. Due to the broadening the output of the close-to-degenerate SPDC process can be split into many channels with the help of external or integrated spectral filters. The inherent possibility of the proposed device heterostructure to achieve and maintain the phase-matching conditions while tuning the pump wavelength in a relatively narrow range is one of the key advantages of the proposed design making it a practical solution for the development of robust and efficient entangled photon pair emitters.

III. INITIAL-VALUE PROBLEM FOR SPDC

Although our ultimate goal is to solve the boundary-value propagation problem for coupled pump, signal, and idler modes in a finite-length laser waveguide, to clarify some universal properties of SPDC here we outline the solution of the initial-value problem, which is much better studied. This will allow us to see which degrees of freedom can be entangled in the intracavity SPDC process, and which ones cannot. The initial-value problem describes SPDC of cavity modes [6,33], especially in high-Q cavities, although in our case the laser waveguide is long and lossy enough for the parametric decay to develop in a single-pass propagation regime.

Consider a dispersive and anisotropic but uniform nonlinear medium of volume V. It is described by the linear permittivity tensor $\overleftrightarrow{\varepsilon}(\omega)$ and the second-order (rank 3) nonlinear susceptibility tensor $\overleftrightarrow{\chi}^{(2)}(\omega_1+\omega_2=\omega_3)$. We are using this double-arrow notation for dielectric response tensors to save the hat notation for quantum-mechanical operators.

Consider the fields at fixed frequencies satisfying the energy conservation in the parametric decay:

$$\omega_p = \omega_V + \omega_H, \tag{1}$$

where the electric field at frequency ω_p is a classical pump field, $\mathbf{E}_p e^{-i\omega_p t+i\mathbf{k}_p\cdot\mathbf{r}}+$ c.c. The Schrödinger operators of the quantum field at frequencies $\omega_{V,H}$ are defined as [34,35]

$$\hat{\mathbf{E}} = \sum_{\mathbf{k}} (\hat{c}_{V\mathbf{k}}\mathbf{E}_{V\mathbf{k}} e^{i\mathbf{k}\cdot\mathbf{r}} + \text{H.c.}) + \sum_{\mathbf{q}} (\hat{c}_{H\mathbf{q}}\mathbf{E}_{H\mathbf{q}} e^{i\mathbf{q}\cdot\mathbf{r}} + \text{H.c.}). \tag{2}$$

Here $\hat{c}_{V\mathbf{k}}$ and $\hat{c}_{H\mathbf{q}}$ are standard bosonic annihilation operators; wave vectors $\mathbf{k}(\omega_V)$ and $\mathbf{q}(\omega_H)$ are determined from the dispersion relations for the eigenwaves with periodic boundary conditions; $\mathbf{E}_{V\mathbf{k}}$ and $\mathbf{E}_{H\mathbf{q}}$ are normalization amplitudes for the fields. The direction of $\mathbf{E}_{V\mathbf{k}}$ and $\mathbf{E}_{H\mathbf{q}}$ corresponds to the polarization of the eigenmodes in the medium with dielectric permittivity tensor $\overleftrightarrow{\varepsilon}(\omega)$. We denote the polarizations by indices V (vertical) and H (horizontal), although the polarization state of the eigenmodes in an anisotropic medium can be more complex [36].

The dispersion equations and polarizations of the normalized field amplitudes in Eq. (2) are found by solving a classical electrodynamics problem, whereas the *magnitudes* of these vector amplitudes have to be determined by field quantization in the volume V [34,35]:

$$\mathbf{E}^*_{V\mathbf{k}} \left\{ \frac{\partial\left[\omega^2 \overleftrightarrow{\varepsilon}(\omega)\right]}{\omega\partial\omega} \right\}_{\omega=\omega_V} \mathbf{E}_{V\mathbf{k}} = \frac{4\pi\hbar\omega_V}{V},$$
$$\mathbf{E}^*_{H\mathbf{q}} \left\{ \frac{\partial\left[\omega^2 \overleftrightarrow{\varepsilon}(\omega)\right]}{\omega\partial\omega} \right\}_{\omega=\omega_H} \mathbf{E}_{H\mathbf{q}} = \frac{4\pi\hbar\omega_H}{V}. \tag{3}$$

The second-order nonlinearity gives rise to three-wave mixing. Exactly at resonance described by Eq. (1) the Hamiltonian of the system in the interaction picture and

rotating-wave approximation takes the form (see, e.g., [37])

$$\hat{H}_{\rm int} = -\sum_{\mathbf{k},\mathbf{q}} (M_{\mathbf{kq}} \hat{c}^{\dagger}_{V\mathbf{k}} \hat{c}^{\dagger}_{H\mathbf{q}} + \text{H.c.}), \tag{4}$$

where

$$M_{\mathbf{kq}} = \mathbf{E}^{*}_{V\mathbf{k}} \overleftrightarrow{\chi}^{(2)}(\omega_p - \omega_H = \omega_V)\mathbf{E}_p\, \mathbf{E}^{*}_{H\mathbf{q}} \times \int_V e^{i[\mathbf{k}_p - \mathbf{k}(\omega_V) - \mathbf{q}(\omega_H)]\cdot\mathbf{r}} d^3 r \tag{5}$$

and

$$\mathbf{E}^{*}_{V\mathbf{k}} \overleftrightarrow{\chi}^{(2)}(\omega_p - \omega_H = \omega_V)\mathbf{E}_p\, \mathbf{E}^{*}_{H\mathbf{q}} = \mathbf{E}^{*}_{H\mathbf{q}} \overleftrightarrow{\chi}^{(2)}(\omega_p - \omega_V = \omega_H)\mathbf{E}_p\, \mathbf{E}^{*}_{V\mathbf{k}} \tag{6}$$

(for the last relationship see, e.g., Chap. 2.9 in [38]).

Now assume that there is only one wave vector $\mathbf{k}$ for each wave vector $\mathbf{q}$ (and vice versa) in the sum $\sum_{\mathbf{k},\mathbf{q}}(\cdots)$ in Eq. (4) for which the phase-matching condition $\mathbf{k}_p(\omega_p) = \mathbf{k}(\omega_V) + \mathbf{q}(\omega_H)$, the energy conservation Eq. (1), and polarization selection rules imposed by the nonlinear susceptibility tensor are satisfied simultaneously. In this case the Hamiltonian of the system can be written as

$$\hat{H}_{\rm int} = \sum_{\mathbf{k},\mathbf{q}} \hat{H}_{\mathbf{kq}}(\hat{c}^{\dagger}_{V\mathbf{k}}, \hat{c}_{V\mathbf{k}}, \hat{c}^{\dagger}_{H\mathbf{q}}, \hat{c}_{H\mathbf{q}}), \tag{7}$$

in which any two terms $\hat{H}_{\mathbf{kq}}$ and $\hat{H}_{\mathbf{k'q'}}$ of the sum have *no common operator*. The operator $\hat{H}_{\mathbf{kq}}$ does not act on the state $|\Psi_{V\mathbf{k}';H\mathbf{q}'}\rangle$, if the pairs of vectors $\mathbf{k}$, $\mathbf{q}$ and $\mathbf{k}'$, $\mathbf{q}'$ are different. Here the notation $|\Psi_{V\mathbf{k};H\mathbf{q}}\rangle$ corresponds to the state vector for two degrees of freedom of the field: the V mode with wave vector $\mathbf{k}$ and the H mode with wave vector $\mathbf{q}$, or signal and idler in the SPDC process.

It is easy to show (see, e.g., [39]) by solving the Schrödinger equation $i\hbar\frac{\partial}{\partial t}|\Psi\rangle = \hat{H}_{\rm int}|\Psi\rangle$ with the Hamiltonian (7) that if the state vector was in a factorized form at the initial moment of time, i.e., $|\Psi(t=0)\rangle = \prod_{\mathbf{k},\mathbf{q}} |\Psi_{V\mathbf{k};H\mathbf{q}}(t=0)\rangle$, it preserves the factorized form:

$$|\Psi(t)\rangle = \prod_{\mathbf{k},\mathbf{q}} e^{-\frac{i}{\hbar}\hat{H}_{\mathbf{kq}}t} |\Psi_{V\mathbf{k};H\mathbf{q}}(t=0)\rangle. \tag{8}$$

Therefore, the state vector for each pair of the signal and idler degrees of freedom $V\mathbf{k}$ and $H\mathbf{q}$ corresponds to their entangled state as they are coupled by the classical pump according to the Hamiltonian (7), but any such pair is not entangled with any other pair. This is the manifestation of the general result: if the Hamiltonian of a system is a sum of the Hamiltonians of the subsystems and the state vector of the system was a product state of the state vectors of the subsystems at the initial moment of time, it will always remain a product state.

For the vacuum initial state $\prod_{\mathbf{k},\mathbf{q}} |0_{V\mathbf{k}}\rangle|0_{H\mathbf{q}}\rangle$ one obtains

$$|\Psi\rangle = \prod_{\mathbf{k},\mathbf{q}} \sum_{n=0}^{\infty} \frac{1}{n!} \left(\frac{i t_{\rm int}}{\hbar}\right)^n (M_{\mathbf{kq}} \hat{c}^{\dagger}_{V\mathbf{k}} \hat{c}^{\dagger}_{H\mathbf{q}} + M^{*}_{\mathbf{kq}} \hat{c}_{V\mathbf{k}} \hat{c}_{H\mathbf{q}})^n \times |0_{V\mathbf{k}}\rangle|0_{H\mathbf{q}}\rangle, \tag{9}$$

where $|0_{V\mathbf{k}}\rangle$ and $|0_{H\mathbf{q}}\rangle$ are vacuum states for the corresponding degrees of freedom and $t_{\rm int}$ is the characteristic time of the SPDC development determined by the interaction length. Within a pure initial-value problem, the value of $t_{\rm int}$ cannot be calculated and has to be estimated from some *ad hoc* considerations. For example if the propagation is along the z axis, the characteristic time can be estimated as $t_{\rm int} \approx \frac{L_z}{\sqrt{\upsilon_{V_z}\upsilon_{H_z}}}$, where υ_{V_z} and υ_{H_z} are the group velocities of the eigenmodes along z and L_z is the propagation length; see the discussion in the end of Appendix A.

To simplify the result we assume the degenerate case when $\omega_V = \omega_H = \omega_p/2$ and the sum in Eq. (4) contains only two pairs of the wave vectors: $\mathbf{k} = \mathbf{k}_1$, $\mathbf{q} = \mathbf{k}_2$ and $\mathbf{k} = \mathbf{k}_2$, $\mathbf{q} = \mathbf{k}_1$. We denote the states corresponding to wave vectors $\mathbf{k}_1$ and $\mathbf{k}_2$ as 1 and 2. One often introduces "intuitive" (although inaccurate) notations $|1_{V1}\rangle|0_{H1}\rangle \Rightarrow |V_1\rangle$, $|1_{H1}\rangle|0_{V1}\rangle \Rightarrow |H_1\rangle$, etc.

Then an *exact* solution in Eq. (9) gives the state vector in the factorized form as

$$|\Psi_{V1;H2;V2;H1}\rangle = |\Psi_{V1;H2}\rangle|\Psi_{V2;H1}\rangle = \left(\sum_{n=0}^{\infty} C_{n(V1)(H2)}|n_{V1}\rangle|n_{H2}\rangle\right) \times \left(\sum_{m=0}^{\infty} C_{m(V2)(H1)}|m_{V2}\rangle|m_{H1}\rangle\right),$$

where $|n_{\ldots}\rangle$ and $|m_{\ldots}\rangle$ are Fock states. It is obvious from the exact solution that the entanglement takes place only within each pair of the degrees of freedom $V1 \Leftrightarrow H2$ and $V2 \Leftrightarrow H1$ (see the sums in parentheses) whereas the states of *different* pairs $|\Psi_{V1;H2}\rangle$ and $|\Psi_{V2;H1}\rangle$ are not entangled. This has been pointed out many times before (e.g., [3,37]). One well-known way to produce polarization-entangled Bell states out of biphoton states generated by type-II SPDC in conventional uniaxial nonlinear crystals is via detecting only the photons coming from the two directions where the ordinary and extraordinary cones overlap, so the "which mode" information is lost [3]. Another approach to creating polarization-entangled Bell states is by linear optical transformations as reviewed, e.g., in [37]. Of course there are many selection and post-selection techniques to achieve the same result. Finally, each photon pair is still entangled with its corresponding vacuum state as $|\Psi_{V1;H2}\rangle \approx |0_{V1}\rangle|0_{H2}\rangle + \frac{i}{\hbar} t_{\rm int} M_{12}|1_{V1}\rangle|1_{H2}\rangle$ (in linear approximation with respect to $t_{\rm int}M_{12}$). This type of correlations can be expressed as the superposition of Bell states $|\Phi^{\pm}_{V1;H2}\rangle = (1/\sqrt{2})(|0_{V1}\rangle|0_{H2}\rangle \pm |1_{V1}\rangle|1_{H2}\rangle)$ and characterized in homodyne detection experiments. Other types of Bell states can be obtained by further processing.

The above analysis is valid only for a classical pump. The decay of the photons of a *quantum* field at frequency ω_p leads to a complete entanglement of all degrees of freedom; see Sec. V and Appendix B.

IV. FINITE WAVEGUIDE: THE BOUNDARY-VALUE PROBLEM FOR HEISENBERG OPERATORS

Now that we reminded the reader of the nature of biphoton states generated in SPDC, we can move closer to the waveguide propagation problem of the parametric decay of a given laser mode. Consider the field propagating along the z axis, with the waveguide cross section of the total area S in the x-y

plane. To calculate the generation rate of two-photon states, we again assume that the laser mode is described by a classical coherent field (the pump):

$$\mathbf{E}_p(\mathbf{r}_\perp)e^{ik_p z - i\omega_p t} + \mathbf{E}_p^*(\mathbf{r}_\perp)e^{-ik_p z + i\omega_p t},$$

where $\mathbf{r}_\perp = (x, y)$.

The quantized waveguide modes within each pair of decay photons have to be of different polarizations, TE and TM type, and satisfy energy conservation similar to Eq. (1):

$$\omega_p = \omega_{\mathrm{TE}} + \omega_{\mathrm{TM}}. \tag{10}$$

In the boundary-value waveguide propagation problem we need to describe the quantized field of decay photons with time- and coordinate-dependent field operators. We will introduce the mode index $N = \mathrm{TE,TM}$ for brevity, which labels both the field polarization and the transverse profile of the field $\mathbf{E}_N(\mathbf{r}_\perp)$. Its dispersion equation is $\omega = \omega_N(k)$. It is convenient to set apart fast space-time oscillations at the optical frequency and wave number, and introduce operators associated with slowly varying field amplitudes:

$$\begin{aligned}\hat{\mathbf{E}}_N = {} & \hat{c}_N(z,t)\mathbf{E}_N(\mathbf{r}_\perp)e^{ik_N(\omega_N)z - i\omega_N t} \\ & + \hat{c}_N^\dagger(z,t)\mathbf{E}_N^*(\mathbf{r}_\perp)e^{-ik_N(\omega_N)z + i\omega_N t}.\end{aligned} \tag{11}$$

The normalization of the field is

$$\int_S \mathbf{E}_N^*(\mathbf{r}_\perp)\left\{\frac{\partial\left[\omega^2 \overleftrightarrow{\varepsilon}(\omega, \mathbf{r}_\perp)\right]}{\omega\partial\omega}\right\}_{\omega=\omega_N} \mathbf{E}_N(\mathbf{r}_\perp)d^2r = 4\pi\hbar\omega_N, \tag{12}$$

where $\overleftrightarrow{\varepsilon}(\omega, \mathbf{r}_\perp)$ is the linear dielectric permittivity tensor. With this definition the dyadic $\hat{c}_N^\dagger(z,t)\hat{c}_N(z,t)$ is the operator of a photon number per unit length along z, which can slowly change with time and z.

To obtain commutation relations for the operators $\hat{c}_N^\dagger(z,t)$ and $\hat{c}_N(z,t)$ we select a segment of the waveguide of length L, such that $\frac{2\pi}{k_N} \ll L \ll L_E$, where L_E is a characteristic scale of the inhomogeneity of the fields along z. The latter inequality allows one to impose periodic boundary conditions in the segment L, perform a standard quantization procedure in it, and go to the limit of a continuous spectrum (see [23,40,41]. As a result, we obtain

$$[\hat{c}_N(z,t), \hat{c}_N(z',t')] = \delta_{NN'}\delta[z - z' - \upsilon_N(t - t')], \tag{13}$$

where $\upsilon_N = \frac{\partial\omega_N}{\partial k}$ is the group velocity. For the particular case $z = z'$ this procedure was used, e.g., in [23,24,40–42]. Note that the commutator (13) is only accurate within slowly varying approximation, in the same way as the notion of the photon number density [34].

When solving boundary-value problems it is usually convenient to use spectral components of the field operators and their commutators at $z = z'$ (see [23,24,40,42]):

$$[\hat{c}_{N\nu}(z), \hat{c}_{N'\nu'}^\dagger(z)] = \delta_{NN'}\frac{\delta(\nu - \nu')}{2\pi\upsilon_N}, \tag{14}$$

where

$$\hat{c}_N(z,t) = \int_{\Delta\omega} \hat{c}_{N\nu}(z)e^{-i\nu t}d\nu, \quad \hat{c}_N^\dagger(z,t) = \int_{\Delta\omega} \hat{c}_{N\nu}^\dagger(z)e^{i\nu t}d\nu, \tag{15}$$

$\Delta\omega$ being the frequency bandwidth occupied by the quantized field. The factor $\frac{1}{2\pi\upsilon_N}$ comes from the density-of-states argument and corresponds to the ratio $\frac{\Delta n_N}{L}$, where Δn_N is the number of states in the interval $d\omega$ when a given mode with index N is quantized within a segment L with periodic boundary conditions. Equations (14) and (15) reflect the fact that the field envelopes occupy a narrow but finite bandwidth.

In this section we use the Heisenberg-Langevin formalism to calculate the evolution of the field operators. We will follow our previous work [23,24,33,39,40,42,43]. The step-by-step derivation for the general nondegenerate SPDC process is in Appendix A. Here we consider only the degenerate SPDC case when $\omega_{\mathrm{TE}} = \omega_{\mathrm{TM}} = \omega_p/2$. We assume that exact phase matching is reached for central frequencies, $k_{\mathrm{TM}}(\frac{\omega_p}{2}) + k_{\mathrm{TE}}(\frac{\omega_p}{2}) - k_p = 0$. The phase mismatch still accumulates with finite detuning ν from the central frequencies, determining the SPDC bandwidth as we see below. Generalizing to an arbitrary phase mismatch and nondegenerate SPDC is straightforward but more cumbersome and the general result is in Appendix A.

A. Heisenberg-Langevin equations for field operators

The coupled equations for the slowly varying field operators are

$$\left(\frac{\partial}{\partial t} + \Gamma_{\mathrm{TE}} + \upsilon_{\mathrm{TE}}\frac{\partial}{\partial z}\right)\hat{c}_{\mathrm{TE}} - \frac{i}{\hbar}A\hat{c}_{\mathrm{TM}}^\dagger = \hat{L}_{\mathrm{TE}}, \tag{16}$$

$$\left(\frac{\partial}{\partial t} + \Gamma_{\mathrm{TM}} + \upsilon_{\mathrm{TM}}\frac{\partial}{\partial z}\right)\hat{c}_{\mathrm{TM}}^\dagger + \frac{i}{\hbar}A^*\hat{c}_{\mathrm{TE}} = \hat{L}_{\mathrm{TM}}^\dagger. \tag{17}$$

Here

$$A = \int_S \mathbf{E}_{\mathrm{TE}}^*(\mathbf{r}_\perp)[\overleftrightarrow{\chi}^{(2)}(\mathbf{r}_\perp)\mathbf{E}_p(\mathbf{r}_\perp)\mathbf{E}_{\mathrm{TM}}^*(\mathbf{r}_\perp)]d^2r, \tag{18}$$

where $\overleftrightarrow{\chi}^{(2)}$ is the second-order nonlinear susceptibility, and $\mathbf{E}_{\mathrm{TE}}^*\overleftrightarrow{\chi}_p^{(2)}\mathbf{E}_p\mathbf{E}_{\mathrm{TM}}^* = \mathbf{E}_{\mathrm{TM}}^*\overleftrightarrow{\chi}_p^{(2)}\mathbf{E}_p\mathbf{E}_{\mathrm{TE}}^*$ [38]. The factors Γ_N determine modal losses for the field and are related to the Langevin noise operators $\hat{L}_N$ through fluctuation-dissipation relations (see [23,24,39,40,42,43]). Equations similar to (16) and (17) which however include the finite phase mismatch are given in Appendix A [see Eqs. (A7) and (A8)].

Following [23,24,42], we will use the following relationships for the Langevin noise operators:

$$[\hat{L}_{N\nu}(z), \hat{L}_{N'\nu'}^\dagger(z')] = \frac{\Gamma_N}{\pi}\delta_{NN'}\delta(\nu - \nu')\delta(z - z'), \tag{19}$$

$$\langle\hat{L}_{N\nu}^\dagger(z)\hat{L}_{N'\nu'}(z')\rangle = \frac{\Gamma_N n_T(\omega_N)}{\pi}\delta_{NN'}\delta(\nu - \nu')\delta(z - z'), \tag{20}$$

where $\langle\cdots\rangle$ means averaging over both an initial quantum state in the Heisenberg picture and the statistics of the dissipative reservoir, $n_T(\omega) = (e^{\hbar\omega/T} - 1)^{-1}$:

$$\hat{L}_N = \int_{\Delta\omega} \hat{L}_{N\nu}e^{-i\nu t}d\nu, \quad \hat{L}_N^\dagger = \int_{\Delta\omega} \hat{L}_{N\nu}^\dagger e^{i\nu t}d\nu.$$

Equation (19) ensures the conservation of the commutation relation Eq. (14) despite the presence of dissipation.

In our previous work [33,43] we developed the version of the Heisenberg-Langevin approach which takes into account

the fluctuations of the field induced by fluctuating currents in the dissipative material or due to the leaking of the external fluctuating field into the waveguide. The effects depend on the effective temperature of corresponding reservoirs. In this paper we assume that the temperatures of the external radiation field and the material which fills the waveguide are much lower than the photon frequencies $\hbar\omega_N$, and it is sufficient to take the value of Γ_N equal to the sum of radiative and Ohmic losses in Eqs. (19) and (20) and take $\hbar\omega/T \to \infty$.

Equations (16) and (17) have the boundary conditions

$$\hat{c}_N(t, z=0) = \hat{c}_N^{(0)}(t). \tag{21}$$

The slow time dependence in $\hat{c}_N^{(0)}$ is due to a finite (although narrow) bandwidth $\Delta\omega$:

$$\hat{c}_N^{(0)}(t) = \int_{\Delta\omega} \hat{c}_{N\nu}^{(0)} e^{-i\nu t} d\nu, \quad \hat{c}_N^{(0)\dagger}(t) = \int_{\Delta\omega} \hat{c}_{N\nu}^{(0)\dagger} e^{i\nu t} d\nu, \tag{22}$$

where $\hat{c}_{N\nu}^{(0)}$ is the Schrödinger (constant) operator. If the field at the boundary is an incoherent noise field with a certain spectral photon distribution $n(\omega)$, the following useful relationships are satisfied:

$$\begin{aligned} \langle \hat{c}_{N\nu}^{(0)\dagger} \hat{c}_{N'\nu'}^{(0)} \rangle &= n(\omega_N)\delta_{NN'} \frac{\delta(\nu-\nu')}{2\pi\, \upsilon_N}, \\ \langle \hat{c}_{N\nu}^{(0)} \hat{c}_{N'\nu'}^{(0)\dagger} \rangle &= [n(\omega_N)+1]\delta_{NN'} \frac{\delta(\nu-\nu')}{2\pi\, \upsilon_N}. \end{aligned} \tag{23}$$

The photon flux in the narrow frequency band $\Delta\omega$ is $Q_N = \upsilon_N \langle \hat{c}_N^{(0)\dagger} \hat{c}_N^{(0)} \rangle = n(\omega_N)\frac{\Delta\omega}{2\pi}$. In particular, for vacuum boundary conditions in Eq. (23) we have $n(\omega_N) = 0$. For a thermal noise we have $n_T(\omega_N) = (e^{\hbar\omega_N/T} - 1)^{-1}$, where T is temperature in energy units. In the Rayleigh-Jeans limit we obtain $Q_N \approx \frac{T\Delta\omega}{2\pi\hbar\omega_i}$. The last expression corresponds to the known result: the radiation power $\frac{T\Delta\omega}{2\pi}$ received by a matched antenna in the blackbody bath does not depend on the size and shape of an aperture.

In the boundary-value problem, it is convenient to transfer from the operators $\hat{c}_N$ which determine the *density* of the photon number per unit length along the waveguide, $\langle \hat{c}_N^\dagger \hat{c}_N \rangle$, to the operators $\hat{a}_N = \sqrt{\upsilon_N}\hat{c}_N$ which determine the *flux* of photons in the waveguide, $\langle \hat{a}_N^\dagger \hat{a}_N \rangle$.

Next, we transfer to the flux operators in Eqs. (16) and (17) and use the Fourier expansion

$$\hat{a}_N(z,t) = \int_{\Delta\omega} \hat{a}_{N\nu} e^{-i\nu t} d\nu, \quad \hat{a}_N^\dagger(z,t) = \int_{\Delta\omega} \hat{a}_{N\nu}^\dagger e^{i\nu t} d\nu. \tag{24}$$

The flux operators $\hat{a}_{N\nu}$ satisfy the commutation relations that follow from Eq. (14), namely,

$$[\hat{a}_{N\nu}(z), \hat{a}_{N'\nu'}^\dagger(z)] = \delta_{NN'} \frac{\delta(\nu-\nu')}{2\pi}. \tag{25}$$

This gives

$$\left(-i\frac{\nu + i\Gamma_{\mathrm{TE}}}{\upsilon_{\mathrm{TE}}} + \frac{\partial}{\partial z}\right)\hat{a}_{\mathrm{TE}\nu} - ig\hat{a}_{\mathrm{TM}(-\nu)}^\dagger = \frac{1}{\sqrt{\upsilon_{\mathrm{TE}}}}\hat{L}_{\mathrm{TE}\nu}(z), \tag{26}$$

$$\left(-i\frac{\nu + i\Gamma_{\mathrm{TM}}}{\upsilon_{\mathrm{TM}}} + \frac{\partial}{\partial z}\right)\hat{a}_{\mathrm{TM}(-\nu)}^\dagger + ig^*\hat{a}_{\mathrm{TE}\nu} = \frac{1}{\sqrt{\upsilon_{\mathrm{TM}}}}\hat{L}_{\mathrm{TM}(-\nu)}^\dagger(z), \tag{27}$$

where the coupling coefficient

$$g = \frac{A}{\hbar\sqrt{\upsilon_{\mathrm{TE}}\upsilon_{\mathrm{TM}}}}. \tag{28}$$

Vacuum boundary conditions for the flux operators follow from Eqs. (23):

$$\begin{aligned} \langle \hat{a}_{\mathrm{TE}\nu}^{(0)\dagger} \hat{a}_{\mathrm{TE}\nu'}^{(0)} \rangle &= \langle \hat{a}_{\mathrm{TM}(-\nu)}^{(0)\dagger} \hat{a}_{\mathrm{TM}(-\nu')}^{(0)} \rangle = 0, \\ \langle \hat{a}_{\mathrm{TE}\nu}^{(0)} \hat{a}_{\mathrm{TE}\nu'}^{(0)\dagger} \rangle &= \langle \hat{a}_{\mathrm{TM}(-\nu)}^{(0)} \hat{a}_{\mathrm{TM}(-\nu')}^{(0)\dagger} \rangle = \frac{\delta(\nu-\nu')}{2\pi} \end{aligned} \tag{29}$$

where $\hat{a}_{N\nu}^{(0)} = \hat{a}_{N\nu}(z=0)$. Similar relationships which take into account phase mismatch are given in Appendix A [see Eqs. (A19) and (A20)].

B. Observable biphoton fluxes

The solution for operators $\hat{a}_{N\nu}$ is given in Appendix A, Eq. (A21) (see similar derivations in [23,24,40]). Here we give the final expressions for the observable spectral fluxes of photons at the cross section $z = L$ of the waveguide. In the absence of coherent incident fields at signal and idler frequencies we have $\langle \hat{a}_{N\nu}^\dagger(z)\hat{a}_{N\nu'}(z)\rangle \propto \delta(\nu-\nu')$. Using the solution for the flux operators from Appendix A for vacuum boundary conditions and Langevin noise given by Eqs. (19) and (20), we arrive at

$$Q_{N\nu}(L) = \int_{\Delta\omega} d\nu' \langle \hat{a}_{N\nu}^\dagger(L)\hat{a}_{N\nu'}(L)\rangle = Q_{N\nu}^{(s)}(L) + Q_{N\nu}^{\mathrm{noise}}(L), \tag{30}$$

where we separated the "signal" component of the flux $Q_{N\nu}^{(s)}$ and the noise component $Q_{N\nu}^{\mathrm{noise}}$ which does not depend on the boundary conditions for the fields:

$$Q_{\mathrm{TE}\nu}^{(s)}(L) = Q_{\mathrm{TM}(-\nu)}^{(s)}(L) = e^{-\left(\frac{\Gamma_{\mathrm{TE}}}{\upsilon_{\mathrm{TE}}} + \frac{\Gamma_{\mathrm{TM}}}{\upsilon_{\mathrm{TM}}}\right)L} \frac{|g|^2}{2\pi} \left| \frac{e^{\kappa L} - e^{-\kappa L}}{2\kappa} \right|^2, \tag{31}$$

$$\begin{pmatrix} Q_{\mathrm{TE}\nu}^{\mathrm{noise}}(L) \\ Q_{\mathrm{TM}(-\nu)}^{\mathrm{noise}}(L) \end{pmatrix} = \begin{pmatrix} \frac{\Gamma_{\mathrm{TM}}}{\upsilon_{\mathrm{TM}}} \\ \frac{\Gamma_{\mathrm{TE}}}{\upsilon_{\mathrm{TE}}} \end{pmatrix} \frac{|g|^2}{4\pi\,|\kappa|^2} F(\mu_\pm, L), \tag{32}$$

where

$$\begin{aligned} F(\mu_\pm, L) = {} & \frac{e^{2\mathrm{Re}[\mu_+]L} - 1}{2\mathrm{Re}[\mu_+]} + \frac{e^{2\mathrm{Re}[\mu_-]L} - 1}{2\mathrm{Re}[\mu_-]} \\ & - 2\mathrm{Re}\left[\frac{e^{(\mu_+^* + \mu_-)L} - 1}{\mu_+^* + \mu_-}\right], \end{aligned} \tag{33}$$

$$\mu_\pm = i\frac{\nu}{2}\left(\frac{1}{\upsilon_{\mathrm{TM}}} + \frac{1}{\upsilon_{\mathrm{TE}}}\right) - \frac{1}{2}\left(\frac{\Gamma_{\mathrm{TM}}}{\upsilon_{\mathrm{TM}}} + \frac{\Gamma_{\mathrm{TE}}}{\upsilon_{\mathrm{TE}}}\right) \pm \kappa, \tag{34}$$

$$\kappa = \sqrt{|g|^2 - \frac{1}{4}\left[D(\nu) + i\left(\frac{\Gamma_{\mathrm{TE}}}{\upsilon_{\mathrm{TE}}} - \frac{\Gamma_{\mathrm{TM}}}{\upsilon_{\mathrm{TM}}}\right)\right]^2}, \tag{35}$$

$$D(\nu) = \nu\left(\frac{1}{\upsilon_{\mathrm{TE}}} - \frac{1}{\upsilon_{\mathrm{TM}}}\right). \tag{36}$$

Here $D(\nu)$ is the phase mismatch for TE and TM modes at frequencies $\frac{\omega_p}{2} + \nu$ and $\frac{\omega_p}{2} - \nu$, respectively. When calculating the noise components of the fluxes we assumed that at

optical frequencies the reservoir can be treated as having zero temperature. In this case we have $n_T(\omega) = 0$ in Eq. (20).

Note that the dynamic components of the fluxes in TE and TM modes are equal to each other even though their absorption losses may be very different; see Eq. (31). This property holds only for vacuum boundary conditions with zero average number of photons. For a classical field or any multiquantum field at the boundary the mode with lower losses will accumulate a higher flux.

The frequency spectrum of the down-converted photons is determined by the dependence $\kappa(\nu)$ in Eqs. (35) and (36). As follows from Eqs. (31), (35), and (36), in the absence of dissipation the parametric amplification occurs in the frequency interval $|D(\nu)| = |\nu(\frac{1}{\upsilon_{\rm TE}} - \frac{1}{\upsilon_{\rm TM}})| < 2|g|$. For $D(\nu) \to 0$ the threshold for parametric amplification is determined by dissipation: $\frac{\Gamma_{\rm TE}\Gamma_{\rm TM}}{\upsilon_{\rm TE}\upsilon_{\rm TM}} < |g|^2$. Taking into account Eq. (28), the last inequality can be written as $\Gamma_{\rm TE}\Gamma_{\rm TM} < \frac{|A|^2}{\hbar^2}$, which is exactly the condition for the parametric amplification in the initial-value problem [33]. In Appendix A these relationships are generalized to the case of finite phase mismatch; see the discussion after Eq. (A27).

As one can see from Eq. (32), the decay photon fluxes "swap" their noise components in the SPDC process: the photon flux in the TE mode is proportional to the absorption coefficient of the TM mode and vice versa. Therefore, when the noise reservoir is at zero temperature, there occurs parametric transfer of quantum noise between the two decay modes while the photon flux of a given mode does not have any contribution from its own noise component. This feature is characteristic of the down-conversion and it illustrates that the contribution of noise always has to be included in the analysis as it is present even at zero temperature of the reservoir. In contrast, one can show that in the *up-conversion* process the Langevin noise does not make any contribution to the up-converted photon flux as long as the reservoir can be treated as having zero temperature for high enough frequencies.

It follows from Eqs. (31)–(33) that the relative contribution of the Langevin noises is negligible in the parametric amplification regime when $|g| \gg \frac{\Gamma_{\rm TE}}{\upsilon_{\rm TE}}, \frac{\Gamma_{\rm TM}}{\upsilon_{\rm TM}}$. Although this limit is unrealistic for monolithic laser devices, we will still give the result for the spectral flux:

$$Q_{{\rm TE}\nu}(L) = Q_{{\rm TM}(-\nu)}(L) \approx \frac{|g|^2 e^{-(\frac{\Gamma_{\rm TE}}{\upsilon_{\rm TE}} + \frac{\Gamma_{\rm TM}}{\upsilon_{\rm TM}})L}}{2\pi|\kappa|^2} \times \begin{cases} \sinh^2(|\kappa|L) & \text{for } D(\nu) < 2|g| \\ \sin^2(|\kappa|L) & \text{for } D(\nu) > 2|g| \end{cases}, \tag{37}$$

where $|\kappa|^2 \approx ||g|^2 - \frac{1}{4}D^2(\nu)|$. Clearly, the flux of down-converted photons is nonzero even outside the parametric amplification bandwidth; however, it decays at large detunings as $\frac{1}{|\kappa|^2}$ and gets absorbed at propagation distances larger than the absorption length.

If the parametric gain is low, $|g| \ll \frac{\Gamma_{\rm TE}}{\upsilon_{\rm TE}}, \frac{\Gamma_{\rm TM}}{\upsilon_{\rm TM}}$, the flux of down-converted photons decays over distances larger than the absorption length at all frequencies. This is the only realistic situation for a laser device, as one can see from the numerical estimates below. The expression for the flux is especially simple for propagation distances shorter than the absorption length, where the noise contribution is insignificant and we obtain

$$Q_{{\rm TE}\nu}(L) = Q_{{\rm TM}(-\nu)}(L) = \frac{|g|^2 \sin^2(|\kappa|L)}{2\pi|\kappa|^2}, \tag{38}$$

where $|\kappa| \approx \frac{1}{2}|D(\nu)|$. These expressions for spectral flux densities have to be integrated over the bandwidth $\Delta\omega$ determined by the detection system to obtain the total flux. The result is in Appendix A, together with an alternative approach to obtain the nonperturbative solution to Eqs. (16) and (17) in the absence of dissipation following the Riemann-Volterra method.

C. Numerical example for intracavity SPDC in the GaSb-based laser

As a specific example, we calculate the performance of the proposed parametric source of biphotons using the device shown in Fig. 1. We consider the degenerate SPDC when the pump wavelength is 2032 nm and the wavelength of TE and TM polarized decay photons is 4064 nm at exact phase matching [see the crossing point of phase-matching curves in Fig. 1(d)]. Assuming conservatively the same value of $|\chi^{(2)}| = 300$ pm/V in all layers, for an intracavity pump power of 1 W and the waveguide width of 10 μm the coupling coefficient g in Eq. (28) which according to Eq. (35) determines the maximum parametric gain is $g \approx 0.24$ cm^{-1}. This number reflects the reduction by about a factor of 10 due to opposite symmetry of the pump and signal modes which leads to partial cancellation in the overlap integral in Eq. (18). The actual cancellation is likely not that strong if the (unknown) variation of the values of $|\chi^{(2)}|$ between different layers is taken into account.

Note that despite exact phase matching at central frequencies the waveguide dispersion leads to significant difference in the group velocities of the TE and TM decay modes: $\upsilon_{\rm TE} \simeq 8.24 \times 10^9$ cm/s, whereas $\upsilon_{\rm TM} \simeq 8.34 \times 10^9$ cm/s. This group velocity mismatch together with the magnitude of the parametric gain control the spectral properties of the generated biphotons.

For the sake of comparison, we start from the ideal case of negligible dissipation. Figure 2 shows the spectral fluxes of the parametric decay photons for different lengths of the device for negligible absorption of the field modes. As follows from Eqs. (A23), (A24), and (31), the parametric amplification occurs in the relatively narrow frequency interval determined by $|\nu| \leqslant |g|(\frac{1}{\upsilon_{\rm TE}} - \frac{1}{\upsilon_{\rm TM}})^{-1}$, or $\frac{\nu}{2\pi} \simeq 0.02$ THz for our parameters. This causes a sharp peak in the flux at low detunings for long enough propagation lengths $|g|L \geqslant 1$. At much larger detunings κ becomes imaginary and scales as $\kappa \sim i\frac{|D(\nu)|}{2}$. In this case the signal flux scales according to Eq. (38) for low losses or short propagation lengths. Therefore, the total SPDC bandwidth defined as the spectral width of its main maximum is determined by $|\kappa|L < \pi$, or

$$|\nu| < \frac{\Delta\omega_{\rm tot}}{2} = \frac{2\pi}{L}\left(\frac{1}{\upsilon_{\rm TE}} - \frac{1}{\upsilon_{\rm TM}}\right)^{-1}, \tag{39}$$

explaining strong dependence on the propagation length in Figs. 2 and 3.

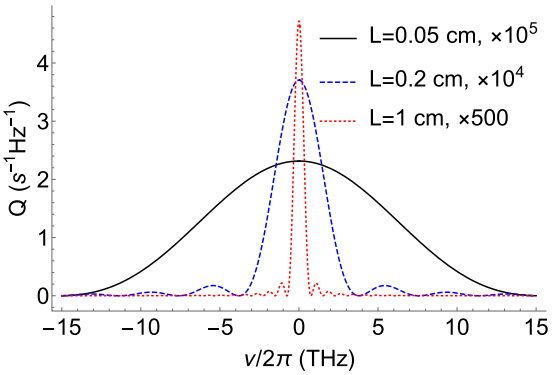

FIG. 2. Spectral flux density of the signal photons given by Eq. (31) for zero absorption losses at three different device lengths: 0.05 cm (black solid line, flux multiplied by 10^5), 0.2 cm (blue dashed line, flux multiplied by 10^4), and 1 cm (red dotted line, flux multiplied by 500). The horizontal axis is the frequency of detuning from resonance $\frac{\nu}{2\pi}$ in THz.

Now we include realistic modal losses and associated noise. Figure 3 shows the spectral fluxes of the parametric decay photons for different lengths of the waveguide and high absorption losses and noise for a laser device: field absorption coefficients $\frac{\Gamma_{\rm TE}}{v_{\rm TE}} = 4\ {\rm cm}^{-1}$ and $\frac{\Gamma_{\rm TM}}{v_{\rm TM}} = 3\ {\rm cm}^{-1}$ (the intensity absorption would be two times higher, 8 and 6 ${\rm cm}^{-1}$). The spectral width of its main maximum which determines the total SPDC bandwidth is given by $|\kappa|L < \pi$, or $|\nu| < \frac{4\pi}{L}(\frac{1}{v_{\rm TE}} - \frac{1}{v_{\rm TM}})^{-1}$. The signal flux is exponentially decreasing for propagation lengths longer than the absorption length, i.e., $(\frac{\Gamma_{\rm TE}}{v_{\rm TE}} + \frac{\Gamma_{\rm TM}}{v_{\rm TM}})L \gg 1$. At the same time, the peak noise flux becomes stronger than the peak signal flux at those lengths. The noise bandwidth is narrower than the signal's. It is determined by the condition $\frac{\Gamma_{\rm TE}}{v_{\rm TE}}, \frac{\Gamma_{\rm TM}}{v_{\rm TM}} \sim \nu(\frac{1}{v_{\rm TE}} - \frac{1}{v_{\rm TM}})$. Therefore, the optimal device length that maximizes the SPDC flux while still avoiding noise throughout most of the SPDC bandwidth is of the order of 1–2 mm, which happens to be also the optimal length for high-performance GaSb-based diode lasers. The total SPDC bandwidth $\frac{\Delta\nu}{2\pi}$ for these lengths is around 10 THz. As one can see from Fig. 3, the signal flux for a 1-mm-long device within the bandwidth of $\frac{\Delta\omega}{2\pi} = 2$ THz near the peak is around 10^8 biphotons/s even for high losses, which makes it interesting for applications, especially for such a small monolithic device. The flux into the total SPDC bandwidth will be several times higher. The peak flux can be further increased by increasing the intracavity pump field intensity and modal overlap, and decreasing modal losses after some design optimization.

D. Fluctuations and correlations between fluxes of decay photons

The above results shed light on the kind of quantum correlations (or entanglement) that could be detected in the decay photon fluxes in the laser output. Suppose that one can detect the photon fluxes with a given polarization (TE or TM) within spectral bands $\Delta\omega_+$ and $\Delta\omega_-$ that are symmetrically located around the central frequency $\frac{\omega_p}{2}$, i.e., they have their central frequencies at $\frac{\omega_p}{2} \pm \delta\omega_0$, and have the frequency bandwidth

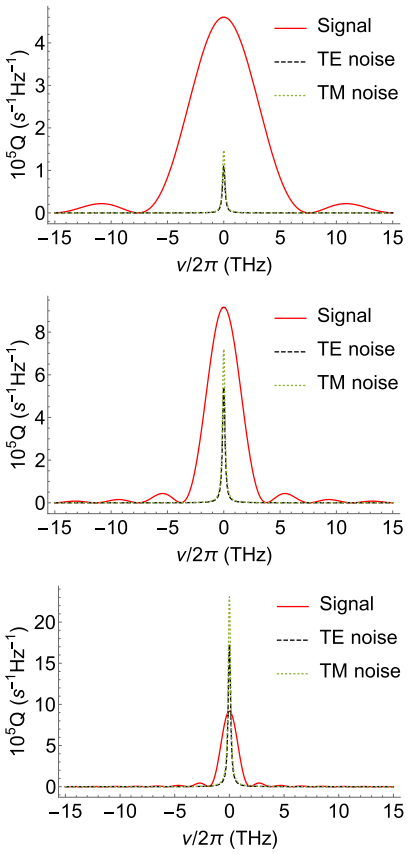

FIG. 3. Spectral flux density of the signal photons given by Eq. (31) (red solid line) and TE and TM polarized noise photons given by Eq. (32) (black dashed line and green dotted line) for the field absorption coefficients $\frac{\Gamma_{\rm TE}}{v_{\rm TE}} = 4\ {\rm cm}^{-1}$ and $\frac{\Gamma_{\rm TM}}{v_{\rm TM}} = 3\ {\rm cm}^{-1}$ at the device length of 1 mm (top panel), 2 mm (middle panel), and 4 mm (bottom panel). All fluxes are multiplied by 10^5. The horizontal axis is the frequency of detuning from resonance $\frac{\nu}{2\pi}$ in THz.

equal to $\Delta\omega$. In other words, the photon fluxes are detected within the frequency intervals $\delta\omega_0 - \frac{\Delta\omega}{2} \leqslant \omega - \frac{\omega_p}{2} \leqslant \delta\omega_0 + \frac{\Delta\omega}{2}$ and $-\delta\omega_0 - \frac{\Delta\omega}{2} \leqslant \omega - \frac{\omega_p}{2} \leqslant -\delta\omega_0 + \frac{\Delta\omega}{2}$, respectively. Note that Eqs. (26) and (27) couple pairwise the following operators of the spectral field harmonics: $\hat{a}_{{\rm TE}\nu}$ with $\hat{a}^\dagger_{{\rm TM}(-\nu)}$ and $\hat{a}_{{\rm TM}(-\nu)}$ with $\hat{a}^\dagger_{{\rm TE}\nu}$, where $\nu = \omega - \frac{\omega_p}{2}$ is defined as the detuning from the central frequency, in the same way as in previous subsections. The fluxes of TE and TM photons *between* the spectral intervals $\Delta\omega_+$ and $\Delta\omega_-$ will be correlated. At the same time, there are no correlations between the photon fluxes with different polarizations *within* each bandwidth $\Delta\omega_+$ or $\Delta\omega_-$.

We can determine the degree of correlations between photon fluxes quantitatively by calculating their correlation function,

$$\mathcal{K}(\tau) = \Big\langle \int_{\Delta\omega_+} \hat{a}^\dagger_{{\rm TE}\nu}\, e^{i\nu(t+\tau)} d\nu \int_{\Delta\omega_+} \hat{a}_{{\rm TE}\nu}\, e^{-i\nu(t+\tau)} d\nu \times \int_{\Delta\omega_-} \hat{a}^\dagger_{{\rm TM}\nu}\, e^{i\nu t} d\nu \int_{\Delta\omega_-} \hat{a}_{{\rm TM}\nu}\, e^{-i\nu t} d\nu \Big\rangle$$

$$-\left\langle \int_{\Delta\omega_+} \hat{a}^\dagger_{\mathrm{TE}\nu}\, e^{i\nu}\, d\nu \int_{\Delta\omega_+} \hat{a}_{\mathrm{TE}\nu}\, e^{-i\nu t}\, d\nu \right\rangle$$
$$\times \left\langle \int_{\Delta\omega_-} \hat{a}^\dagger_{\mathrm{TM}\nu}\, e^{i\nu t}\, d\nu \int_{\Delta\omega_-} \hat{a}_{\mathrm{TM}\nu}\, e^{-i\nu t}\, d\nu \right\rangle, \quad (40)$$

and comparing it with fluctuations of each flux, given by

$$\mathcal{D}_N = \left\langle \left(\int_{\Delta\omega_\pm} \hat{a}^\dagger_{N\nu}\, e^{i\nu t}\, d\nu \int_{\Delta\omega_\pm} \hat{a}_{N\nu}\, e^{-i\nu t}\, d\nu \right)^2 \right\rangle$$
$$- \left\langle \int_{\Delta\omega_\pm} \hat{a}^\dagger_{N\nu}\, e^{i\nu t}\, d\nu \int_{\Delta\omega_\pm} \hat{a}_{N\nu}\, e^{-i\nu t}\, d\nu \right\rangle^2. \quad (41)$$

Here $N = \mathrm{TE,TM}$ correspond to the top and bottom sign in $\Delta\omega_\pm$, respectively.

The dimensionless parameter characterizing the degree of correlations at the waveguide output L is

$$\Theta(L,\tau) = \frac{\mathcal{K}(L,\tau)}{\sqrt{\mathcal{D}_{\mathrm{TE}}(L)\mathcal{D}_{\mathrm{TM}}(L)}}. \quad (42)$$

It reaches the maximum value of 1 for completely correlated fluxes, and is smaller than 1 otherwise. The correlation time for the photon fluxes is just an inverse of the detection bandwidth, i.e., it is $\approx 1/\Delta\omega_{\mathrm{tot}}$ if the photons are detected over the whole SPDC bandwidth in Eq. (39) and it is of the order of $1/\Delta\omega$ for a narrower bandwidth.

All terms on the right-hand side of Eq. (42) can be calculated from the solution for the flux operators $\hat{a}_{N\nu}(L)$ obtained in Appendix A. For an optimal case, we choose the frequency intervals $\Delta\omega_\pm$ outside the Langevin noise band in Fig. 3, when $D(\nu) \gg \frac{\Gamma_{\mathrm{TE}}}{\upsilon_{\mathrm{TE}}}, \frac{\Gamma_{\mathrm{TM}}}{\upsilon_{\mathrm{TM}}}$, and we can neglect the terms dependent on the the Langevin operators in the expressions for $\hat{a}_{N\nu}$. Using the equality $\langle 0|\hat{a}^\dagger_{N\nu}(0)\hat{a}_{N\nu'}(0)\hat{a}^\dagger_{N\nu''}(0)\hat{a}_{N\nu'''}(0)|0\rangle = 0$ and the commutation relation Eq. (25) one can obtain

$$\mathcal{D}_{\mathrm{TE}}(L) = Q^{(s)}_{\mathrm{TE}}(L) e^{-(\frac{\Gamma_{\mathrm{TE}}}{\upsilon_{\mathrm{TE}}}+\frac{\Gamma_{\mathrm{TM}}}{\upsilon_{\mathrm{TM}}})L} \frac{|g|^2}{2\pi}$$
$$\times \int_{\Delta\omega} d\nu \left| \frac{e^{\kappa L}K_- - e^{-\kappa L}K_+}{2\kappa} \right|^2, \quad (43)$$

$$\mathcal{D}_{\mathrm{TM}}(L) = Q^{(s)}_{\mathrm{TM}}(L) e^{-(\frac{\Gamma_{\mathrm{TE}}}{\upsilon_{\mathrm{TE}}}+\frac{\Gamma_{\mathrm{TM}}}{\upsilon_{\mathrm{TM}}})L} \frac{|g|^2}{2\pi}$$
$$\times \int_{\Delta\omega} d\nu \left| \frac{e^{\kappa L}K_+ - e^{-\kappa L}K_-}{2\kappa} \right|^2, \quad (44)$$

and

$$\mathcal{K}(L) = e^{-2(\frac{\Gamma_{\mathrm{TE}}}{\upsilon_{\mathrm{TE}}}+\frac{\Gamma_{\mathrm{TM}}}{\upsilon_{\mathrm{TM}}})L} \frac{|g|^4}{4\pi^2} \left| \int_{\Delta\omega} d\nu\, e^{-i\nu\tau} \right.$$
$$\left. \times \frac{(e^{\kappa L}K_- - e^{-\kappa L}K_+)(e^{\kappa^* L} - e^{-\kappa^* L})}{|2\kappa|^2} \right|^2, \quad (45)$$

where the functions $\kappa(\nu)$ and $K_\pm(\nu)$ are given by Eqs. (A23)–(A25) whereas the values of fluxes $Q^{(s)}_{\mathrm{TE,TM}}(L)$ are determined by integrating the flux spectral densities in Eq. (31) over the spectral bandwidth.

In our example of a dissipative laser waveguide $|g| \ll \frac{\Gamma_{\mathrm{TE}}}{\upsilon_{\mathrm{TE}}}, \frac{\Gamma_{\mathrm{TM}}}{\upsilon_{\mathrm{TM}}}$, in which case $\kappa \simeq i|\kappa|$ and $K_\pm \simeq \frac{-D(\nu)}{2g} \pm \frac{|\kappa|}{g}$ where one can without loss of generality assume that g is real. This leads to further simplification of the above integrals, in which

$$e^{\kappa L}K_- - e^{-\kappa L}K_+ \simeq -i\frac{D(\nu)}{g}\sin(|\kappa|L) - \frac{2|\kappa|}{g}\cos(|\kappa|L),$$
$$e^{\kappa L}K_+ - e^{-\kappa L}K_- \simeq -i\frac{D(\nu)}{g}\sin(|\kappa|L) + \frac{2|\kappa|}{g}\cos(|\kappa|L).$$

It is straightforward to calculate that if the signal bandwidths are selected narrow enough as compared to the total SPDC bandwidth defined in Eq. (39), namely,

$$\Delta\omega \ll \Delta\omega_{\mathrm{tot}} = \frac{4\pi}{L}\left(\frac{1}{\upsilon_{\mathrm{TE}}} - \frac{1}{\upsilon_{\mathrm{TM}}}\right)^{-1}, \quad (46)$$

the photon fluxes at the output facet of a waveguide $z = L$ have a maximum possible correlation: $\Theta(L, \tau = 0) = 1$. With increasing signal bandwidth the maximum correlation is reduced below 1 and its peak is shifted towards nonzero time delays. This behavior is illustrated in Fig. 4.

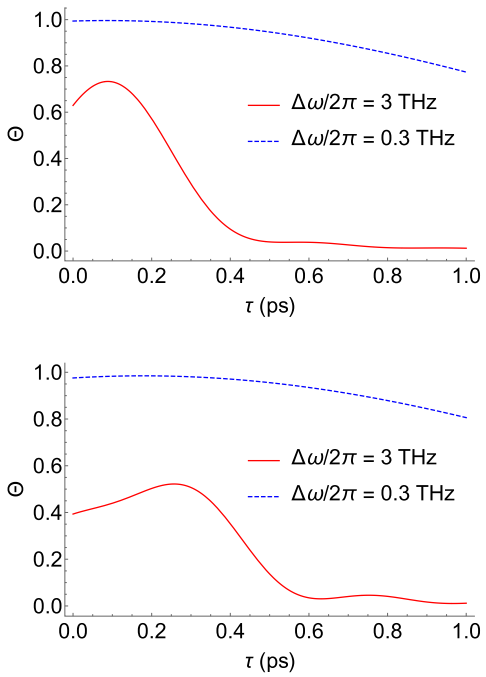

FIG. 4. The correlation parameter $\Theta(L,\tau)$ as a function of time delay τ for waveguide length $L = 1$ mm (top panel) and $L = 2$ mm (bottom panel). The plots on each panel are for two values of signal bandwidths: $\frac{\Delta\omega}{2\pi} = 3$ THz (red solid line) and $\frac{\Delta\omega}{2\pi} = 0.3$ THz (blue dashed line). The frequency detuning of the signal bandwidth center from the central frequency $\frac{\omega_p}{2}$ is $\frac{\delta\omega_0}{2\pi} = 6$ THz for the top panel and 3 THz for the bottom panel.

Figure 4 shows the correlation parameter $\Theta(L,\tau)$ as a function of time delay τ for two waveguide lengths, $L = 1$ and 2 mm, which correspond to the average flux spectra shown in Fig. 3, top and middle panel, respectively. For these two waveguide lengths we took the center frequencies of the detection bandwidths shifted by $\frac{\delta\omega_0}{2\pi} = \pm 6$ or ± 3 THz, respectively, from the central frequency $\frac{\omega_p}{2}$. Clearly, for a narrow signal bandwidth $\frac{\Delta\omega}{2\pi} = 0.3$ THz the correlation is close to its maximum value of 1 over time delays shorter than $\approx 1/\Delta\omega$. This is true for both device lengths. When the signal bandwidth becomes comparable in magnitude to the total SPDC band-

width, the correlations degrade and the peak is shifted. This is more pronounced for a $L = 2$ mm device which has the total SPDC bandwidth $\frac{\Delta\omega_{\rm tot}}{2\pi} = 7.6$ THz, as compared to a shorter, $L = 1$ mm device which has the total SPDC bandwidth of 15.2 THz.

The displacement of the maximum in Fig. 4 is due to the difference between the arrival times of the photons traveling with different group velocities. The inequality (46), which ensures that the maximum correlation function is reached at zero delay, has a simple interpretation: it means that the correlation time $\tau_{\rm corr} \approx \frac{2\pi}{\Delta\omega}$ of the signal detected in each mode is much longer than the difference between the arrival times of the photons with different group velocities, $\Delta\tau \approx L(\frac{1}{\upsilon_{\rm TE}} - \frac{1}{\upsilon_{\rm TM}})$. In this case the effect of group velocity difference is unimportant and the maximum correlation is reached at $\tau \approx 0$. When the correlation time $\tau_{\rm corr}$ approaches the group delay time $\Delta\tau$, the maximum of the correlation function is shifted to nonzero delays.

V. BOUNDARY-VALUE PROBLEM FOR THE SCHRÖDINGER EQUATION

In the boundary-value problem solved in the previous section, the observables are determined using a constant Heisenberg-picture state vector $|\Psi(t=0)\rangle$ at the boundary $z = 0$. Within the same approximation one can also introduce the notion of a space-dependent state vector which would be equivalent to the space evolution of Heisenberg operators. With this goal in mind, let us look at Eqs. (26) and (27) for the spectral components of the field operators neglecting for simplicity the Langevin noise and dissipation. Since these equations contain only spatial derivatives, taking into account the commutation relations (25) for $\hat{a}_{N\nu}$ one can write the "lossless" version of Eqs. (26) and (27) and their Hermitian conjugates as "spatial" versions of the Heisenberg equations, namely,

$$\frac{\partial}{\partial z}\hat{O} = \frac{i}{\hbar}[\hat{H}_{\rm eff}, \hat{O}], \tag{47}$$

where $\hat{O} = \hat{a}_{{\rm TE}\nu}, \hat{a}^\dagger_{{\rm TE}\nu}, \hat{a}_{{\rm TM}(-\nu)}, \hat{a}^\dagger_{{\rm TM}(-\nu)}$ and

$$\hat{H}_{\rm eff} = 2\pi\hbar\left\{\int d\nu \frac{\nu}{\upsilon_{\rm TE}}\hat{a}^\dagger_{{\rm TE}\nu}\hat{a}_{{\rm TE}\nu} + \int d\nu \frac{\nu}{\upsilon_{\rm TM}}\hat{a}^\dagger_{{\rm TM}\nu}\hat{a}_{{\rm TM}\nu} - \iint d\nu d\nu' \delta(\nu+\nu')(g\hat{a}^\dagger_{{\rm TE}\nu}\hat{a}^\dagger_{{\rm TM}\nu'} + {\rm H.c.})\right\}. \tag{48}$$

Note that the operator $\hat{H}_{\rm eff}$ in Eq. (47) generates translations along z, not time, and therefore it has the dimension of momentum.

The formal solution to Eq. (47) has a standard form:

$$\hat{O}(z) = e^{\frac{i}{\hbar}\hat{H}_{\rm eff}z}\hat{O}(0)e^{-\frac{i}{\hbar}\hat{H}_{\rm eff}z}.$$

Note that one can represent in this way the z dependence for any combination of operators, $\hat{O}(z) \Rightarrow (\hat{a}_{{\rm TE}\nu})^n \quad (\hat{a}^\dagger_{{\rm TE}\nu})^l(\hat{a}_{{\rm TM}(-\nu)})^p(\hat{a}^\dagger_{{\rm TM}(-\nu)})^s$. After requesting that the following condition be met, $\langle\Psi(0)|\hat{O}(z)|\Psi(0)\rangle = \langle\Psi(z)|\hat{O}(0)|\Psi(z)\rangle$, we arrive at

$$|\Psi(z)\rangle = e^{-\frac{i}{\hbar}\hat{H}_{\rm eff}z}|\Psi(0)\rangle,$$

which gives the space evolution equation for the state vector:

$$i\hbar\frac{\partial}{\partial z}|\Psi\rangle = \hat{H}_{\rm eff}|\Psi\rangle. \tag{49}$$

Equation (49) is quite intuitive and could be postulated from the very beginning as was done, e.g., in [44]. However, this *ad hoc* approach considers the decay into a single mode. In our case the parametric decay occurs into two different modes with different polarizations and group velocities, which plays a principal role in all aspects of SPDC as we saw above. It is also not clear without the derivation of how to relate the empirical coupling coefficient between modes to the actual $\chi^{(2)}(r)$ and modal parameters.

For the classical pumping field there is no real need in using Eq. (49) because the Heisenberg equations (26) and (27) are linear and can be easily solved. The situation is different when the pumping field is quantized too, for example if it is given by

$$\hat{\mathbf{E}}_p = \hat{c}_p(z,t)\mathbf{E}_p(\mathbf{r}_\perp)e^{ik_p(\omega_p)z - i\omega_p t} + \hat{c}^\dagger_p(z,t)\mathbf{E}^*_p(\mathbf{r}_\perp)e^{-ik_p(\omega_p)z + i\omega_p t}, \tag{50}$$

where $\mathbf{E}_p(\mathbf{r}_\perp)$ is the normalization amplitude given by Eq. (12) where one should replace subscript N with p.

Instead of Eqs. (26) and (27) we now obtain

$$-i\frac{\nu}{\upsilon_{\rm TE}}\hat{a}_{{\rm TE}\nu} + \frac{\partial}{\partial z}\hat{a}_{{\rm TE}\nu} = iG\iint d\nu' d\nu'' \delta(\nu+\nu'-\nu'')\hat{a}_{p\nu''}\hat{a}^\dagger_{{\rm TM}\nu'}, \tag{51}$$

$$i\frac{\nu'}{\upsilon_{\rm TM}}\hat{a}^\dagger_{{\rm TM}\nu'} + \frac{\partial}{\partial z}\hat{a}^\dagger_{{\rm TM}\nu'} = -iG^*\iint d\nu d\nu'' \delta(\nu+\nu'-\nu'')\hat{a}^\dagger_{p\nu''}\hat{a}_{{\rm TE}\nu}, \tag{52}$$

$$-i\frac{\nu''}{\upsilon_p}\hat{a}_{p\nu''} + \frac{\partial}{\partial z}\hat{a}_{p\nu''} = iG^*\iint d\nu d\nu' \delta(\nu+\nu'-\nu'')\hat{a}_{{\rm TE}\nu}\hat{a}_{{\rm TM}\nu'}, \tag{53}$$

where $\hat{a}_{p\nu''} = \sqrt{\upsilon_p}\hat{c}_{p\nu''}$, υ_p is the group velocity of the pump mode, and

$$G = \frac{\int_S \mathbf{E}^*_{\rm TE}(\mathbf{r}_\perp)[\overleftrightarrow{\chi}^{(2)}(\mathbf{r}_\perp)\mathbf{E}_p(\mathbf{r}_\perp)\mathbf{E}^*_{\rm TM}(\mathbf{r}_\perp)]d^2r}{\hbar\sqrt{\upsilon_{\rm TE}\upsilon_{\rm TM}\upsilon_p}}. \tag{54}$$

Equations (51)–(53) correspond to the Heisenberg-like equation (47) with effective "Hamiltonian"

$$\hat{H}_{\rm eff} = 2\pi\hbar\left[\int d\nu \frac{\nu}{\upsilon_{\rm TE}}\hat{a}^\dagger_{{\rm TE}\nu}\hat{a}_{{\rm TE}\nu} + \int d\nu \frac{\nu}{\upsilon_{\rm TM}}\hat{a}^\dagger_{{\rm TM}\nu}\hat{a}_{{\rm TM}\nu} + \int d\nu \frac{\nu}{\upsilon_p}\hat{a}^\dagger_{p\nu}\hat{a}_{p\nu} - \iiint d\nu d\nu' d\nu'' \delta(\nu+\nu'-\nu'') \times (G\hat{a}_{p\nu''}\hat{a}^\dagger_{{\rm TE}\nu}\hat{a}^\dagger_{{\rm TM}\nu'} + {\rm H.c.})\right], \tag{55}$$

i.e., one can again arrive at the equation of the type of Eq. (49), but with the Hamiltonian (55). The difference however is that now the operator-valued equations (51)–(53) are nonlinear whereas Eq. (49) for the state vector is always linear. This

is a crucial advantage of the approach based on Eq. (49). It is important that Eq. (49) can be generalized for open systems with dissipation and fluctuation effects using the stochastic equation for the state vector [45,46], and the method of quantum jumps [20,47]. Here we illustrate our approach with an example of an external flux of pump photons propagating in a passive waveguide. Obviously, an active lasing device considered in the previous sections cannot produce a single-photon pump flux.

To avoid cumbersome derivations, we will switch from the continuous spectrum to a discrete set of frequencies; see, e.g., Ch. 10 in [48]. This approach requires renormalization of the operators $\hat{a}_{N\nu}$, where $N = \mathrm{TE,TM}$, or p. The quantities $\langle \hat{a}^\dagger_{N\nu}\hat{a}_{N\nu}\rangle$ are now the total fluxes of photons of a given polarization within a given spectral line, i.e., they have the dimension of $\sec^{-1}$. This renormalization of the operators is easiest to illustrate with an example of the parametric decay of a quasimonochromatic pump mode at frequency ω_p with bandwidth $\Delta\omega \ll \omega_p$. The spectrum of signal and idler photons is convenient to represent as a set of discrete spectral lines at frequencies $\frac{\omega_p}{2} + \nu$, where ν spans a discrete set of values symmetric with respect to $\omega_p/2$ and each spectral line has the same width $\Delta\omega$. The renormalized operators satisfy the commutation relations that follow from Eq. (25) (see also the Supplemental Material in [40]):

$$[\hat{a}_{N\nu}, \hat{a}^\dagger_{N'\nu'}] = \frac{\Delta\omega}{2\pi}\delta_{NN'}\delta_{\nu\nu'}, \tag{56}$$

where for $N = p$ the only option is $\nu = 0$. Therefore, one can introduce standard states of the boson field:

$$\sqrt{\frac{2\pi}{\Delta\omega}}\hat{a}_{N\nu}|n_{N\nu}\rangle = \sqrt{n_{N\nu}}|(n-1)_{N\nu}\rangle,$$
$$\sqrt{\frac{2\pi}{\Delta\omega}}\hat{a}^\dagger_{N\nu}|n_{N\nu}\rangle = \sqrt{(n+1)_{N\nu}}|(n+1)_{N\nu}\rangle. \tag{57}$$

The discrete version of the effective Hamiltonian to be used in Eq. (49) is

$$\hat{H}_{\mathrm{eff}} = \frac{2\pi\hbar}{\Delta\omega}\sum_\nu\left[\frac{\nu}{v_{\mathrm{TE}}}\hat{a}^\dagger_{\mathrm{TE}\nu}\hat{a}_{\mathrm{TE}\nu} + \frac{\nu}{v_{\mathrm{TM}}}\hat{a}^\dagger_{\mathrm{TM}\nu}\hat{a}_{\mathrm{TM}\nu} - (G\hat{a}_p\hat{a}^\dagger_{\mathrm{TE}\nu}\hat{a}^\dagger_{\mathrm{TM}(-\nu)} + \mathrm{H.c.})\right]. \tag{58}$$

It is easy to verify that substituting $\hat{H}_{\mathrm{eff}}$ from Eq. (58) into Eq. (47) and taking into account the commutation relations (56) will give a correct "discrete" version of Eqs. (51)–(53) [see Eqs. (B1)–(B3) in Appendix B].

When the state vector is expressed in terms of these number states as $\Psi_{N\nu} = \sum_n C^{(n)}_{N\nu}(z)|n\rangle$, the quantities $|C^{(n)}_{N\nu}(z)|^2$ have the meaning of the probability to detect the flux of photons $\langle \hat{a}^\dagger_{N\nu}\hat{a}_{N\nu}\rangle = Q_0 n$ at the cross section z, where $Q_0 = \frac{\Delta\omega}{2\pi}$. The quantity $\hbar\omega_N Q_0$ is the energy flux transported by a single photon with waveform of duration $\frac{2\pi}{\Delta\omega}$. The bandwidth $\Delta\omega$ and the values of the amplitudes $C^{(n)}_{N\nu}(z=0)$ at the boundary are determined by the properties of the pump. Therefore, within the discrete approach we need to assign a certain spectral bandwidth $\Delta\omega$ to the pump field, which is defined by externally controlled properties of the pump, and to split the spectrum of decay photons into the spectral lines of the same width. We are not considering a rather exotic situation in which the "allowed" spectral bands for the signal and idler photons have to be narrower than the pump field bandwidth.

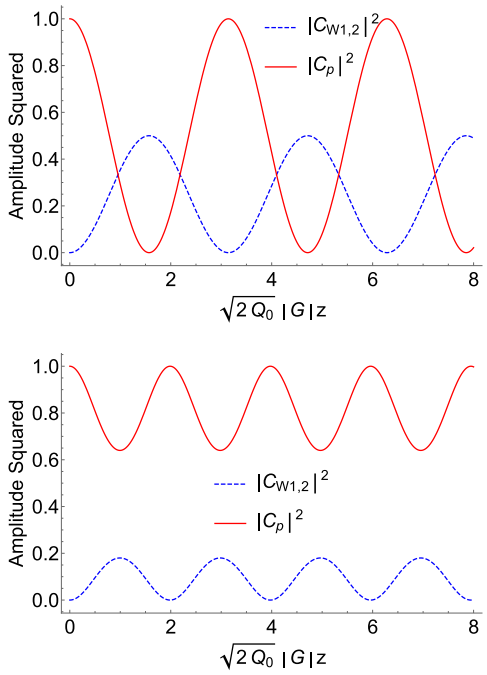

FIG. 5. Occupation probabilities $|C_p(z)|^2$ (red solid line) and $|C_{W1}(z)|^2$ and $|C_{W2}(z)|^2$ (blue dashed line) as a function of the normalized propagation distance z along the waveguide for $\delta = 0$ (top panel) and $\delta = 3\sqrt{2Q_0}|G|$ (bottom panel). The plots for $|C_{W1}(z)|^2$ and $|C_{W2}(z)|^2$ are identical.

Consider a parametric decay when the quantum state at the boundary is $|\Psi(0)\rangle = |1_p\rangle|0_{\mathrm{TE,TM}}\rangle$, where $|0_{\mathrm{TE,TM}}\rangle$ is a vacuum state of the signal and idler photons at all frequencies. In this case the solution to Eq. (49) must have the form

$$|\Psi\rangle = C_p(z)|1_p\rangle|0_{\mathrm{TE,TM}}\rangle + \sum_\nu C_{W\nu}(z)|0_p\rangle|1_{\mathrm{TE}\nu}\rangle|1_{\mathrm{TM}(-\nu)}\rangle \times \prod_{\nu'\neq\nu,\nu''\neq-\nu}|0_{\mathrm{TE}\nu'}\rangle|0_{\mathrm{TM}\nu''}\rangle. \tag{59}$$

All other states are forbidden by energy conservation. Equation (59) is the generalization of a tripartite entangled state of the Greenberger-Horne-Zeilinger (GHZ) type [45,49–52]. Note that such states can be also produced in four-wave mixing via a pumped $\chi^{(3)}$ nonlinearity which creates an effective second-order nonlinearity for three coupled quantum modes; see [53] where they also use conversion of a single-photon state into entangled signal and idler states, similarly to our initial conditions.

It is straightforward to solve coupled ordinary differential equations for the coefficients resulting from substituting Eq. (59) into Eq. (49) with the Hamiltonian (58). The detailed derivation is in Appendix B. Figure 5 illustrates the solution when the parametric decay of the pump occurs into photon pairs within only two symmetric spectral bands $\frac{\omega_p}{2} \pm \nu$, where ν has only one value.

The figure shows z dependence of the occupation probabilities $|C_p(z)|^2$, $|C_{W1}(z)|^2$, and $|C_{W2}(z)|^2$ of the photon states $|1_p\rangle|0_{\mathrm{TE,TM}}\rangle$, $|0_p\rangle|1_{\mathrm{TE}\nu}\rangle|0_{\mathrm{TM}\nu}\rangle|0_{\mathrm{TE}(-\nu)}\rangle|1_{\mathrm{TM}(-\nu)}\rangle$, and $|0_p\rangle|0_{\mathrm{TE}\nu}\rangle|1_{\mathrm{TM}\nu}\rangle|1_{\mathrm{TE}(-\nu)}\rangle|0_{\mathrm{TM}(-\nu)}\rangle$, respectively. The periodic modulation of the occupation probabilities with z is a spatial analog of Rabi oscillations, in which the Rabi wave number K_R for the probability amplitudes is given by

$$K_R^2 = \delta^2 + 2Q_0|G|^2, \tag{60}$$

where the detuning

$$\delta = \nu\left(\frac{1}{\upsilon_{\mathrm{TM}}} - \frac{1}{\upsilon_{\mathrm{TE}}}\right). \tag{61}$$

For zero detuning from the central frequencies, at some values of z there is a complete transfer of energy from the single-photon state of the pump to an entangled state of the decay photons. With increasing detuning the modulation occurs with a shorter spatial period according to Eq. (60) and the transfer of excitation is incomplete: it occurs with decreasing probability. Note that the coefficients $C_{W1}(z)$ and $C_{W2}(z)$ have the same amplitudes, although they may have different phases.

By comparing the expression (28) for g in the previous section with the expression for the Rabi wave number $K_R = \sqrt{2Q_0}|G|$ at zero detuning, one can verify that when the power of the classical pumping field in Eq. (28) is equal to the power in the quantized single-photon flux $\hbar\omega_p\frac{\Delta\omega}{2\pi}$, the expressions for K_R and g coincide, which is an important verification of the consistency of the two formalisms.

Numerically, for the same waveguide design as in Fig. 1 one obtains $G \simeq 10^{-10}\ \mathrm{s}^{1/2}\,\mathrm{cm}^{-1}$. Assuming the bandwidth $\frac{\Delta\omega}{2\pi} = 1$ THz the value of K_R is very small, $K_R \sim 10^{-4}\ \mathrm{cm}^{-1}$. This means that the probability of one incident pump photon to decay into the signal and idler photons after propagating the waveguide length of 1 cm is 10^{-4}. Multiplying it by the flux of incident pump photons per second, one can obtain the expected flux of decay biphotons.

Here we considered the parametric decay into two relatively narrow spectral bands. For a broadband decay with the total width of the SPDC spectrum $\Delta\Omega \gg \Delta\omega$, one can split the overall SPDC bandwidth into many narrow bands and perform the summation over these bands in the resulting expression for C_p using, e.g., the method developed in [54] for strong coupling in the systems with inhomogeneous broadening of the spectra; see Appendix B for the derivation details. It is enough to calculate the expression for $C_p(z)$, since other amplitudes $C_{W\nu}(z)$ can be expressed through $C_p(z)$. Note that our results will not depend on the way we split the total bandwidth, i.e., on the parameter $\Delta\omega$.

The general behavior of the solution for the probability amplitudes is controlled by the parameter $\alpha = \frac{\sqrt{\Delta\Omega}}{|G|}|\frac{1}{\upsilon_{\mathrm{TM}}} - \frac{1}{\upsilon_{\mathrm{TE}}}|$. When $\alpha \ll 1$, the solution for $C_p(z)$ is qualitatively similar to the one in the case of a parametric decay into two symmetric narrow lines as long as $\delta \ll \sqrt{2Q_0}|G|$; see Fig. 5. All occupation probabilities $|C_{W\nu}(z)|^2$ are the same and they are related to $|C_p(z)|^2$ by conservation of the photon flux: $|C_p(z)|^2 + \sum_\nu |C_{W\nu}(z)|^2 = 1$. The Rabi wave number which describes spatial oscillations is given by

$$K_R \approx |G|\sqrt{\frac{\Delta\Omega}{2\pi}}. \tag{62}$$

Since for two symmetric bands we have $\Delta\Omega = 2\Delta\omega$, Eq. (62) coincides with Eq. (60) in the limit of small δ.

For the waveguide parameters shown in Fig. 1, we are in the regime corresponding to the opposite limit $\alpha \gg 1$. In this case the dephasing due to spectral broadening dominates and the probability amplitude $C_p(z)$ decays exponentially along z with an exponent:

$$\kappa \simeq \frac{|G|^2}{2}\frac{1}{|\frac{1}{\upsilon_{\mathrm{TM}}} - \frac{1}{\upsilon_{\mathrm{TE}}}|}. \tag{63}$$

The attenuation rate 2κ of the occupation probability due to spectral broadening is $\approx 10^{-8}\ \mathrm{cm}^{-1}$, indicating a very low rate of biphoton production, as expected for a single-photon pump.

VI. CONCLUSIONS

In conclusion, we advanced the quantum theory of the SPDC of eigenmodes in finite-length semiconductor waveguides which takes into account not only all propagation effects such as phase and group velocity mismatch but also, most importantly, the effects of dissipation and quantum and thermal noise. The latter effects are crucial to include in the design of any monolithic semiconductor quantum device and in fact any emerging quantum photonic circuits that are based on lossy materials with high nonlinearity. For example, we show that for the SPDC process the quantum noise makes a significant and even dominant contribution within the signal and idler bandwidth even at low ambient temperature. Any experiment aimed at creating monolithic sources of quantum light has to take coupling to noisy reservoirs into account. Our paper provides the theoretical foundation and convenient analytic formulas to accomplish that.

We applied our formalism to propose and evaluate the performance of a high-brightness, ultracompact electrically pumped laser source of entangled photons generated by intracavity SPDC of lasing modes. The specific design in the paper is based on the III-Sb heterostructure and operation in the atmospheric transparency window of 3–5-μm wavelengths. However, the same device concept can be applied to any III-V material system at other wavelengths.

We developed an approach based on the propagation equation for the state vector which solves the nonperturbative boundary-value problem of the parametric decay of a *quantized* single-photon pump mode and can include the effects of dissipation and noise. Our formalism is applicable to a wide variety of nonlinear wave mixing propagation problems in which all fields are quantized. It unifies the SPDC process with the strong-coupling regime of cavity QED. The parametric strong coupling between three or more degrees of freedom leads to the formation of tripartite entangled states with many applications in quantum information and connections to other areas in quantum optics.

ACKNOWLEDGMENTS

The authors are grateful to Maria Erukhimova for helpful discussions. This work has been supported in part by NSF Grants No. 2135083 and No. 1936276, and by Texas A&M University through Strategic Transformative Research Program, X-grant, and T3-grant programs. M.T. acknowledges

support by Center of Excellence "Center of Photonics", Contract No. 075-15-2020-906.

APPENDIX A: DERIVATIONS FOR SEC. IV OF THE MAIN PAPER: THE BOUNDARY-VALUE PROBLEM FOR HEISENBERG OPERATORS

Here we derive the equations that describe evolution of the operators $\hat{c}_N(z,t)$ which determine the quantized field of decay photons. We use the mode index $N = \text{TE,TM}$ for brevity, which labels both the field polarization and the transverse profile of the field $\mathbf{E}_N(\mathbf{r}_\perp)$. Its dispersion equation is $\omega = \omega_N(k)$. The normalization of the field is defined in Sec. IV of the main paper; see Eq. (15) there.

The field operators for both quantized modes obey the wave equation

$$\frac{\partial^2}{\partial t^2}(\hat{\varepsilon}\hat{\mathbf{E}}) + c^2\nabla\times\nabla\times\hat{\mathbf{E}} = -4\pi\frac{\partial^2}{\partial t^2}\delta\hat{\mathbf{P}} \tag{A1}$$

where

$$\hat{\varepsilon}\hat{\mathbf{E}} = \int_0^\infty \overleftrightarrow{\varepsilon}(\mathbf{r},\tau)\hat{\mathbf{E}}(\mathbf{r},t-\tau)d\tau,$$

$\hat{\varepsilon}$ is a linear Hermitian operator, and $\int_0^\infty \overleftrightarrow{\varepsilon}(\mathbf{r}_\perp,\tau)e^{i\omega\tau}d\tau = \overleftrightarrow{\varepsilon}(\omega,\mathbf{r}_\perp)$ is the dielectric tensor for a nonuniform medium with frequency dispersion. The operator

$$\delta\hat{\mathbf{P}} = \delta\hat{\mathbf{P}}_{\text{diss}} + \delta\hat{\mathbf{P}}_L + \delta\hat{\mathbf{P}}_{\text{NL}} \tag{A2}$$

includes the part describing linear dissipation (since we take as $\hat{\varepsilon}$ Hermitian), the noise component of the polarization, and the nonlinear polarization.

Within the slowly varying amplitude approximation, Eq. (A1) is reduced to

$$\frac{\partial}{\partial t}\hat{c}_N + \upsilon_N\frac{\partial}{\partial z}\hat{c}_N + \Gamma_N\hat{c}_N = \hat{L}_N + \frac{i}{\hbar}e^{i[\kappa_N - k_N(\omega_N)]z}\int_S \mathbf{E}_N^*(\mathbf{r}_\perp)\delta\hat{\mathbf{P}}_{\text{NL};N}(\mathbf{r}_\perp,t,z)d^2r. \tag{A3}$$

Here

$$\delta\hat{\mathbf{P}}_{\text{NL}} = \sum_{N=\text{TE,TM}}[\delta\hat{\mathbf{P}}_{\text{NL};N}(\mathbf{r}_\perp,t,z)e^{i\kappa_N z - i\omega_N t} + \delta\hat{\mathbf{P}}^\dagger_{\text{NL};N}(\mathbf{r}_\perp,t,z)e^{-i\kappa_N z + i\omega_N t}], \tag{A4}$$

where $\delta\hat{\mathbf{P}}_{\text{NL};N}$ is the operator of the nonlinear polarization at frequency ω_N; Γ_N determines modal losses and is related to the Langevin noise operator $\hat{L}_N$ through fluctuation-dissipation relations (see [23,24,39,40,42,43]). Following [23,24,42], we will use the following relationships for the Langevin noise operator:

$$[\hat{L}_{N\nu}(z),\hat{L}^\dagger_{N'\nu'}(z')] = \frac{\Gamma_N}{\pi}\delta_{NN'}\delta(\nu-\nu')\delta(z-z'), \tag{A5}$$

$$\langle\hat{L}^\dagger_{N\nu}(z)\hat{L}_{N'\nu'}(z')\rangle = \frac{\Gamma_N n_T(\omega_N)}{\pi}\delta_{NN'}\delta(\nu-\nu')\delta(z-z'), \tag{A6}$$

where $\langle\cdots\rangle$ means averaging over both an initial quantum state in the Heisenberg picture and the statistics of the dissipative reservoir, $n_T(\omega) = (e^{\hbar\omega/T}-1)^{-1}$:

$$\hat{L}_N = \int_{\Delta\omega}\hat{L}_{N\nu}e^{-i\nu t}d\nu,\quad \hat{L}^\dagger_N = \int_{\Delta\omega}\hat{L}^\dagger_{N\nu}e^{i\nu t}d\nu.$$

Equation (A5) ensures the conservation of the commutation relations [Eq. (14) of the main paper] despite the presence of dissipation.

Besides energy conservation [Eq. (10) of the main paper] one has to satisfy the momentum conservation (phase-matching) condition

$$|k_p(\omega_p) - k_{\text{TE}}(\omega_{\text{TE}}) - k_{\text{TM}}(\omega_{\text{TM}})|L \ll 1,$$

where L is the length of the SPDC region, in the simplest case the laser waveguide length. For our device geometry (see Fig. 1) the combination of energy and momentum conservation at a given pump frequency ω_p can be satisfied for two pairs of frequencies ω_{TE} and ω_{TM} [Fig. 1(d)]. There is also one value of frequency ω_p for which the frequencies of decay photons become equal, $\omega_{\text{TE}} = \omega_{\text{TM}} = \omega_p/2$. We will consider degenerate and nondegenerate SPDC separately.

1. Nondegenerate case: The space-time propagation problem and the perturbation method

Here we assume that the spectral widths of decay photons $\approx \Delta\omega$ determined by phase-matching bandwidth are much lower than the distance between their central frequencies: $\Delta\omega \ll |\omega_{\text{TE}} - \omega_{\text{TM}}|$.

The resulting operator-valued equations for the two modes making up the entangled two-photon state at the output are

$$\frac{\partial}{\partial t}\hat{c}_{\text{TE}} + \upsilon_{\text{TE}}\frac{\partial}{\partial z}\hat{c}_{\text{TE}} + \Gamma_{\text{TE}}\hat{c}_{\text{TE}} = \hat{L}_{\text{TE}} + \frac{i}{\hbar}e^{-i(k_{\text{TM}}+k_{\text{TE}}-k_p)z}A\hat{c}^\dagger_{\text{TM}}, \tag{A7}$$

$$\frac{\partial}{\partial t}\hat{c}^\dagger_{\text{TM}} + \upsilon_{\text{TM}}\frac{\partial}{\partial z}\hat{c}^\dagger_{\text{TM}} + \Gamma_{\text{TM}}\hat{c}^\dagger_{\text{TM}} = \hat{L}^\dagger_{\text{TM}} - \frac{i}{\hbar}e^{i(k_{\text{TM}}+k_{\text{TE}}-k_p)z}A^*\hat{c}_{\text{TE}}. \tag{A8}$$

Here the parameter A is determined in Eq. (18).

To start with the simplest case, we assume that the length L of the decay region is smaller than all absorption lengths $\frac{\upsilon_N}{\Gamma_N}$. This allows us to neglect dissipative and Langevin terms:

$$\frac{\partial}{\partial t}\hat{c}_{\text{TE}} + \upsilon_{\text{TE}}\frac{\partial}{\partial z}\hat{c}_{\text{TE}} = \frac{i}{\hbar}e^{-i(k_{\text{TM}}+k_{\text{TE}}-k_p)z}A\hat{c}^\dagger_{\text{TM}}, \tag{A9}$$

$$\frac{\partial}{\partial t}\hat{c}^\dagger_{\text{TM}} + \upsilon_{\text{TM}}\frac{\partial}{\partial z}\hat{c}^\dagger_{\text{TM}} = -\frac{i}{\hbar}e^{i(k_{\text{TM}}+k_{\text{TE}}-k_p)z}A^*\hat{c}_{\text{TE}}. \tag{A10}$$

When treating the degenerate SPDC in the next subsection, we will consider arbitrary propagation lengths and fully include the effects of dissipation and noise.

The formal solutions to Eqs. (A9) and (A10) are

$$\hat{c}_{\rm TE} = \hat{c}^{(0)}_{\rm TE}\Big(t - \frac{z}{v_{\rm TE}}\Big) + \frac{i}{\hbar}\frac{A}{v_{\rm TE}}\int_0^z e^{-i(k_{\rm TM}+k_{\rm TE}-k_p)\zeta}\hat{c}^{\dagger}_{\rm TM}\Big(t - \frac{z-\zeta}{v_{\rm TE}}, \zeta\Big)d\zeta, \tag{A11}$$

$$\hat{c}^{\dagger}_{\rm TM} = \hat{c}^{(0)\dagger}_{\rm TM}\Big(t - \frac{z}{v_{\rm TM}}\Big) - \frac{i}{\hbar}\frac{A^*}{v_{\rm TM}}\int_0^z e^{i(k_{\rm TM}+k_{\rm TE}-k_p)\zeta}\hat{c}_{\rm TE}\Big(t - \frac{z-\zeta}{v_{\rm TM}}, \zeta\Big)d\zeta, \tag{A12}$$

where

$$\hat{c}_{\rm TE}\Big(t - \frac{z-\zeta}{v_{\rm TM}}, \zeta\Big) = \hat{c}_{\rm TE}(t,z)_{\{t\Rightarrow t-\frac{z-\zeta}{v_{\rm TM}}\ z\Rightarrow\zeta\}}, \quad \hat{c}^{\dagger}_{\rm TM}\Big(t - \frac{z-\zeta}{v_{\rm TE}}, \zeta\Big) = \hat{c}^{\dagger}_{\rm TM}(t,z)_{\{t\Rightarrow t-\frac{z-\zeta}{v_{\rm TE}}\ z\Rightarrow\zeta\}}.$$

Within the perturbation expansion in terms of the coupling parameter A we substitute unperturbed operators given by the first terms in the right-hand side of Eqs. (A11) and (A12) (which describe the transfer of the boundary conditions with the group velocity) into the integrands in Eqs. (A11) and (A12), namely,

$$\hat{c}_{\rm TE}\Big(t - \frac{z-\zeta}{v_{\rm TM}}, \zeta\Big) \Rightarrow \hat{c}^{(0)}_{\rm TE}\Big(t - \frac{z}{v_{\rm TM}} + \zeta\frac{v_{\rm TM}-v_{\rm TE}}{v_{\rm TE}v_{\rm TM}}\Big), \quad \hat{c}^{\dagger}_{\rm TM}\Big(t - \frac{z-\zeta}{v_{\rm TE}}, \zeta\Big) \Rightarrow \hat{c}^{(0)\dagger}_{\rm TM}\Big(t - \frac{z}{v_{\rm TE}} + \zeta\frac{v_{\rm TM}-v_{\rm TE}}{v_{\rm TE}v_{\rm TM}}\Big).$$

This gives

$$\hat{c}_{\rm TE}(t,z) = \hat{c}^{(0)}_{\rm TE}\Big(t - \frac{z}{v_{\rm TE}}\Big) + \frac{i}{\hbar}\frac{A}{v_{\rm TE}}\int_0^z e^{-i(k_{\rm TM}+k_{\rm TE}-k_p)\zeta}\hat{c}^{(0)\dagger}_{\rm TM}\Big(t - \frac{z}{v_{\rm TE}} + \zeta\frac{v_{\rm TM}-v_{\rm TE}}{v_{\rm TE}v_{\rm TM}}\Big)d\zeta, \tag{A13}$$

$$\hat{c}^{\dagger}_{\rm TM}(t,z) = \hat{c}^{(0)\dagger}_{\rm TM}\Big(t - \frac{z}{v_{\rm TM}}\Big) - \frac{i}{\hbar}\frac{A^*}{v_{\rm TM}}\int_0^z e^{i(k_{\rm TM}+k_{\rm TE}-k_p)\zeta}\hat{c}^{(0)}_{\rm TE}\Big(t - \frac{z}{v_{\rm TM}} + \zeta\frac{v_{\rm TM}-v_{\rm TE}}{v_{\rm TE}v_{\rm TM}}\Big)d\zeta. \tag{A14}$$

Expressions (A13) and (A14) allow us to calculate any experimental observables. For example, we can calculate the photon fluxes within the bandwidth $\Delta\omega$ in the cross section $z = L$ for vacuum boundary conditions:

$$Q_{\rm TE} = v_{\rm TE}\langle\hat{c}^{\dagger}_{\rm TE}(L)\hat{c}_{\rm TE}(L)\rangle \approx \frac{\Delta\omega}{2\pi}\frac{|A|^2}{\hbar^2 v_{\rm TE}v_{\rm TM}}\Big|\int_0^L e^{i(k_{\rm TM}+k_{\rm TE}-k_p)z}dz\Big|^2, \tag{A15}$$

$$Q_{\rm TM} = v_{\rm TM}\langle\hat{c}^{\dagger}_{\rm TM}(L)\hat{c}_{\rm TM}(L)\rangle = Q_{\rm TE}. \tag{A16}$$

The last equality corresponds to Manley-Rowe relations [55]. The expression (A15) is valid when the bandwidth $\Delta\omega$ satisfies $L\Delta\omega|\frac{1}{v_{\rm TE}} - \frac{1}{v_{\rm TM}}| \ll 1$.

Using the spectral decomposition of the field operators given by Eqs. (17) of the main paper, one can obtain the solutions for the spectral amplitudes beyond the perturbation approach. We will present such a solution for the degenerate case below, because this is the most interesting case for most applications.

2. Degenerate case: The nonperturbative solution for spectral amplitudes

Consider now the degenerate SPDC when $\omega_{\rm TE} = \omega_{\rm TM} = \omega_p/2$. We start with the most general case when there is still finite phase mismatch δk at central frequencies $\omega_{\rm TE} = \omega_{\rm TM} = \omega_p/2$, namely,

$$k_{\rm TM}\Big(\frac{\omega_p}{2}\Big) + k_{\rm TE}\Big(\frac{\omega_p}{2}\Big) - k_p(\omega_p) = \delta k,$$

and the field dissipation and Langevin noises cannot be neglected. The coupled equations for the field operators are

$$\Big(\frac{\partial}{\partial t} + \Gamma_{\rm TE} + v_{\rm TE}\frac{\partial}{\partial z}\Big)\hat{c}_{\rm TE} - \frac{i}{\hbar}A\hat{c}^{\dagger}_{\rm TM}e^{-i\delta kz} = \hat{L}_{\rm TE}, \tag{A17}$$

$$\Big(\frac{\partial}{\partial t} + \Gamma_{\rm TM} + v_{\rm TM}\frac{\partial}{\partial z}\Big)\hat{c}^{\dagger}_{\rm TM} + \frac{i}{\hbar}A^*\hat{c}_{\rm TE}e^{i\delta kz} = \hat{L}^{\dagger}_{\rm TM}. \tag{A18}$$

Next, we transfer to the flux operators in Eqs. (A17) and (A18) which were introduced in Sec. III A and use the Fourier expansion (24). To get rid of the explicit z dependence in the left-hand sides of Eqs. (A17) and (A18) we make the substitution $\hat{a}^{\dagger}_{\rm TM(-\nu)} = \hat{\tilde{a}}^{\dagger}_{\rm TM(-\nu)}e^{i\frac{\delta k}{2}z}$, $\hat{a}_{\rm TE\nu} = \hat{\tilde{a}}_{\rm TE\nu}e^{-i\frac{\delta k}{2}z}$. This results in

$$\Big(-i\frac{\nu + i\Gamma_{\rm TE}}{v_{\rm TE}} - i\frac{\delta k}{2} + \frac{\partial}{\partial z}\Big)\hat{\tilde{a}}_{\rm TE\nu} - ig\hat{\tilde{a}}^{\dagger}_{\rm TM(-\nu)} = \frac{1}{\sqrt{v_{\rm TE}}}\hat{L}_{\rm TE\nu}(z)e^{-i\frac{\delta k}{2}z}, \tag{A19}$$

$$\Big(-i\frac{\nu + i\Gamma_{\rm TM}}{v_{\rm TM}} + i\frac{\delta k}{2} + \frac{\partial}{\partial z}\Big)\hat{\tilde{a}}^{\dagger}_{\rm TM(-\nu)} + ig^*\hat{\tilde{a}}_{\rm TE\nu} = \frac{1}{\sqrt{v_{\rm TM}}}\hat{L}^{\dagger}_{\rm TM(-\nu)}(z)e^{i\frac{\delta k}{2}z}. \tag{A20}$$

The solution of Eqs. (A19) and ((A20)) can be written as (see the similar derivations in [23,40])

$$\begin{pmatrix}\hat{a}_{\rm TE\nu}(z)\\ \hat{a}^{\dagger}_{\rm TM(-\nu)z}\end{pmatrix} = e^{\mu_+ z}\begin{pmatrix}e^{-i\frac{\delta k}{2}z}\\ e^{i\frac{\delta k}{2}z}K_+\end{pmatrix}\Big(\hat{U}_+ + \int_0^z e^{-\mu_+\xi}\hat{F}_+(\xi)d\xi\Big) + e^{\mu_- z}\begin{pmatrix}e^{-i\frac{\delta k}{2}z}\\ e^{i\frac{\delta k}{2}z}K_-\end{pmatrix}\Big(\hat{U}_- + \int_0^z e^{-\mu_-\xi}\hat{F}_-(\xi)d\xi\Big), \tag{A21}$$

where

$$\mu_{\pm} = i\frac{\nu}{2}\left(\frac{1}{\upsilon_{\rm TM}} + \frac{1}{\upsilon_{\rm TE}}\right) - \frac{1}{2}\left(\frac{\Gamma_{\rm TM}}{\upsilon_{\rm TM}} + \frac{\Gamma_{\rm TE}}{\upsilon_{\rm TE}}\right) \pm \kappa, \quad \text{(A22)}$$

$$\kappa = \sqrt{|g|^2 - \frac{1}{4}\left[D(\nu) + i\left(\frac{\Gamma_{\rm TE}}{\upsilon_{\rm TE}} - \frac{\Gamma_{\rm TM}}{\upsilon_{\rm TM}}\right)\right]^2}, \quad \text{(A23)}$$

$$D(\nu) = \delta k + \nu\left(\frac{1}{\upsilon_{\rm TE}} - \frac{1}{\upsilon_{\rm TM}}\right), \quad \text{(A24)}$$

$$K_{\pm} = \frac{-D(\nu) - i\left(\frac{\Gamma_{\rm TE}}{\upsilon_{\rm TE}} - \frac{\Gamma_{\rm TM}}{\upsilon_{\rm TM}}\right)}{2g} \mp i\frac{\kappa}{g}, \quad \text{(A25)}$$

$$\hat{U}_{\pm} = \pm\frac{g}{i2\kappa}[\hat{a}_{{\rm TE}\nu}(0)K_{\mp} - \hat{a}^{\dagger}_{{\rm TM}(-\nu)}(0)], \quad \text{(A26)}$$

$$\hat{F}_{\pm}(\xi) = \pm\frac{g}{i2\kappa}\left[K_{\mp}\frac{1}{\sqrt{\upsilon_{\rm TE}}}\hat{L}_{{\rm TE}\nu}(\xi)e^{-i\frac{\delta k}{2}\xi} - \frac{1}{\sqrt{\upsilon_{\rm TM}}}\hat{L}^{\dagger}_{{\rm TM}(-\nu)}(\xi)e^{i\frac{\delta k}{2}\xi}\right]. \quad \text{(A27)}$$

Here $D(\nu)$ is the phase mismatch for TE and TM modes at frequencies $\frac{\omega_p}{2} + \nu$ and $\frac{\omega_p}{2} - \nu$, respectively. The square root in Eq. (A23) should be taken as $\sqrt{Z} = \sqrt{|Z|}e^{i\frac{1}{2}{\rm Arg}[Z]}$. It follows from Eq. (A25) that $K_+K_- = e^{-2i{\rm Arg}[g]}$.

The frequency spectrum of the down-converted photons is determined by the dependence $\kappa(\nu)$ in Eqs. (A23) and (A24). As follows from Eqs. (A21), (A23), and (A24), in the absence of dissipation the parametric amplification occurs in the frequency interval $|D(\nu)| = |\delta k + \nu(\frac{1}{\upsilon_{\rm TE}} - \frac{1}{\upsilon_{\rm TM}})| < 2|g|$.

In the absence of dissipation and detuning, i.e., when $\Gamma_{\rm TE} = \Gamma_{\rm TM} = D(\nu) = 0$, the spatial coefficient of amplification is $|g| = \frac{A}{\hbar\sqrt{\upsilon_{\rm TE}\upsilon_{\rm TM}}}$, whereas the growth rate in time for an associated initial-value problem is $\gamma = \frac{|A|}{\hbar}$; see, e.g., [33]. The relationship $|g| = \frac{\gamma}{\sqrt{\upsilon_{\rm TE}\upsilon_{\rm TM}}}$ allows one to express the characteristic time of parametric interaction $t_{\rm int}$ through the parametric amplification length L_z as $t_{\rm int} = \frac{L_z}{\sqrt{\upsilon_{\rm TE}\upsilon_{\rm TM}}}$ which was used in Sec. III of the main paper.

When the detection bandwidth $\Delta\omega$ is narrow enough, namely, $\Delta\omega\frac{|\upsilon_{\rm TE}-\upsilon_{\rm TM}|}{2\upsilon_{\rm TE}\upsilon_{\rm TM}} \ll |g| \approx \kappa$ (i.e., the detection bandwidth is narrower than the parametric amplification bandwidth), after neglecting dissipation and noise and assuming $\delta k = 0$ the solution in Eq. (A21) can be easily summed over frequencies. Returning to the operators $\hat{c}_N$ we obtain

$$\hat{c}_{\rm TE}(z,t) = \hat{c}^{(0)}_{\rm TE}\left(t - \frac{\upsilon_{\rm TE}+\upsilon_{\rm TM}}{2\upsilon_{\rm TE}\upsilon_{\rm TM}}z\right)\cosh(\kappa z) + ie^{i\phi}\sqrt{\frac{\upsilon_{\rm TM}}{\upsilon_{\rm TE}}}\hat{c}^{(0)\dagger}_{\rm TM}\left(t - \frac{\upsilon_{\rm TE}+\upsilon_{\rm TM}}{2\upsilon_{\rm TE}\upsilon_{\rm TM}}z\right)\sinh(\kappa z), \quad \text{(A28)}$$

$$\hat{c}_{\rm TM}(z,t) = \hat{c}^{(0)}_{\rm TM}\left(t - \frac{\upsilon_{\rm TE}+\upsilon_{\rm TM}}{2\upsilon_{\rm TE}\upsilon_{\rm TM}}z\right)\cosh(\kappa z) + ie^{i\phi}\sqrt{\frac{\upsilon_{\rm TE}}{\upsilon_{\rm TM}}}\hat{c}^{(0)\dagger}_{\rm TE}\left(t - \frac{\upsilon_{\rm TE}+\upsilon_{\rm TM}}{2\upsilon_{\rm TE}\upsilon_{\rm TM}}z\right)\sinh(\kappa z), \quad \text{(A29)}$$

where $\phi = {\rm Arg}[g]$.

We can find an exact nonperturbative solution to Eqs. (A17) and (A18) for negligible Langevin noise, losses, and phase mismatch $\Gamma_{\rm TE} = \Gamma_{\rm TM} = \delta k = 0$ in a different way if we notice that after the substitution $x = z - \upsilon_{\rm TE}t$ and $y = z - \upsilon_{\rm TM}t$ they are reduced to the hyperbolic equation

$$\left[\frac{\partial^2}{\partial x\partial y} + \frac{1}{\hbar^2}\frac{|A|^2}{(\upsilon_{\rm TE}-\upsilon_{\rm TM})^2}\right]\Phi = 0,$$

where $\Phi = \hat{c}_{\rm TE}, \hat{c}^{\dagger}_{\rm TM}$. Its solution can be written in quadratures following the Riemann-Volterra method; see, e.g., Chap. 10.3-6 in [56]. However, the solution method based on the Fourier transformation which we used is more convenient in this case. Indeed, it gives us an explicit equation for the SPDC frequency bandwidth and highlights the correlations between the spectral photon fluxes in different frequency bins. Furthermore, the spectral approach provides a straightforward way of including finite phase mismatch, Langevin noise, and absorption losses [see Eqs. (A21)–(A23)]. The spectral method also makes it straightforward to incorporate the quantum dynamics of the reservoir noise (e.g., squeezing) for a finite temperature of the reservoir [24].

APPENDIX B: DERIVATIONS FOR SEC. V OF THE MAIN PAPER: THE BOUNDARY-VALUE PROBLEM FOR THE SCHRÖDINGER EQUATION

To avoid cumbersome derivations, we will switch from the continuous spectrum to a discrete set of frequencies; see, e.g., [48]. We consider the parametric decay of a quasimonochromatic pump mode at frequency ω_p. The spectrum of signal and idler photons is convenient to represent as a set of discrete spectral lines at frequencies $\frac{\omega_p}{2} + \nu$, where ν spans a discrete set of values symmetric with respect to $\omega_p/2$. In this case Eqs. (51)–(53) transform into

$$-i\frac{\nu}{\upsilon_{\rm TE}}\hat{a}_{{\rm TE}\nu} + \frac{\partial}{\partial z}\hat{a}_{{\rm TE}\nu} = iG\hat{a}_p\hat{a}^{\dagger}_{{\rm TM}(-\nu)}, \quad \text{(B1)}$$

$$i\frac{(-\nu)}{\upsilon_{\rm TM}}\hat{a}^{\dagger}_{{\rm TM}(-\nu)} + \frac{\partial}{\partial z}\hat{a}^{\dagger}_{{\rm TM}(-\nu)} = -iG^*\hat{a}^{\dagger}_p\hat{a}_{{\rm TE}\nu}, \quad \text{(B2)}$$

$$\frac{\partial}{\partial z}\hat{a}_p = iG^*\sum_{\nu}\hat{a}_{{\rm TE}\nu}\hat{a}_{{\rm TM}(-\nu)}. \quad \text{(B3)}$$

In Eq. (B3) we assume that $\nu = 0$ is the only option for the pump field and we define $\hat{a}_{p,\nu=0} = \hat{a}_p$.

The transition from Eqs. (51)–(53) to Eqs. (B1)–(B3) corresponds to the renormalization of the operators $\hat{a}_{N\nu}$. The quantities $\langle\hat{a}^{\dagger}_{N\nu}\hat{a}_{N\nu}\rangle$ in Eqs. (B1)–(B3) are now the total fluxes of photons of a given polarization within a given spectral line, i.e., they have the dimension of $\sec^{-1}$. The operators defined in this way satisfy the commutation relations that follow from Eq. (25) (see also the Supplemental Material in [40]):

$$[\hat{a}_{N\nu}, \hat{a}^{\dagger}_{N'\nu'}] = \frac{\Delta\omega}{2\pi}\delta_{NN'}\delta_{\nu\nu'}. \quad \text{(B4)}$$

The Heisenberg equations (B1)–(B3) with commutation relations (B4) correspond to Eqs. (57) and the discrete version of the effective Hamiltonian in Eq. (58).

Substituting Eq. (59) into Eq. (49) with the effective Hamiltonian (58) leads to the following equations for the coefficients:

$$\frac{\partial}{\partial z}C_p = -iG^*\sqrt{\frac{\Delta\omega}{2\pi}}\sum_{\nu} C_{W\nu}, \tag{B5}$$

$$\frac{\partial}{\partial z}C_{W\nu} = i\delta_\nu C_{W\nu} - iG\sqrt{\frac{\Delta\omega}{2\pi}}C_p, \tag{B6}$$

where

$$\delta_\nu = \nu\left(\frac{1}{\upsilon_{\mathrm{TM}}} - \frac{1}{\upsilon_{\mathrm{TE}}}\right). \tag{B7}$$

Let us assume for simplicity that the nonlinear waveguide allows the parametric decay of the pump into photon pairs within only two symmetric spectral bands $\frac{\omega_p}{2} \pm \nu$, where ν has only one value. In this case the solution should be sought in the form

$$\begin{aligned}|\Psi\rangle = {} & C_p(z)|1_p\rangle|0_{\mathrm{TE}\nu}\rangle|0_{\mathrm{TM}\nu}\rangle|0_{\mathrm{TE}(-\nu)}\rangle|0_{\mathrm{TM}(-\nu)}\rangle \\ & + C_{W1}(z)|0_p\rangle|1_{\mathrm{TE}\nu}\rangle|0_{\mathrm{TM}\nu}\rangle|0_{\mathrm{TE}(-\nu)}\rangle|1_{\mathrm{TM}(-\nu)}\rangle \\ & + C_{W2}(z)|0_p\rangle|0_{\mathrm{TE}\nu}\rangle|1_{\mathrm{TM}\nu}\rangle|1_{\mathrm{TE}(-\nu)}\rangle|0_{\mathrm{TM}(-\nu)}\rangle.\end{aligned} \tag{B8}$$

Equations (B5)–(B7) become

$$\frac{\partial}{\partial z}C_p = -iG^*\sqrt{\frac{\Delta\omega}{2\pi}}(C_{W1} + C_{W2}), \tag{B9}$$

$$\frac{\partial}{\partial z}C_{W1} = i\delta C_{W1} - iG\sqrt{\frac{\Delta\omega}{2\pi}}C_p, \tag{B10}$$

$$\frac{\partial}{\partial z}C_{W2} = -i\delta C_{W2} - iG\sqrt{\frac{\Delta\omega}{2\pi}}C_p, \tag{B11}$$

where

$$\delta = \nu\left(\frac{1}{\upsilon_{\mathrm{TM}}} - \frac{1}{\upsilon_{\mathrm{TE}}}\right) \tag{B12}$$

and ν has only one positive value.

The solution for the initial conditions $C_p = 1, C_{W1,2} = 0$ is

$$C_{W1} = -i\frac{G\sqrt{Q_0}}{K_R}\left[\sin K_R z - i\frac{\delta}{K_R}(\cos K_R z - 1)\right], \tag{B13}$$

$$C_{W2} = -i\frac{G\sqrt{Q_0}}{K_R}\left[\sin K_R z + i\frac{\delta}{K_R}(\cos K_R z - 1)\right], \tag{B14}$$

$$C_p = \frac{\delta^2}{K_R^2} + \frac{2Q_0|G|^2}{K_R^2}\cos K_R z \tag{B15}$$

where $Q_0 = \sqrt{\frac{\Delta\omega}{2\pi}}$ and

$$K_R^2 = \delta^2 + 2Q_0|G|^2, \tag{B16}$$

where K_R is the Rabi wave number, introduced in analogy with the Rabi frequency.

The resulting state vector is

$$\begin{aligned}|\Psi\rangle = {} & \left(\frac{\delta^2}{K_R^2} + \frac{2Q_0|G|^2}{K_R^2}\cos K_R z\right)|1_p\rangle|0_{\mathrm{TE}\nu}\rangle|0_{\mathrm{TM}\nu}\rangle|0_{\mathrm{TE}(-\nu)}\rangle|0_{\mathrm{TM}(-\nu)}\rangle - i\frac{G\sqrt{Q_0}}{K_R}\left[\sin K_R z - i\frac{\delta}{K_R}(\cos K_R z - 1)\right] \\ & \times|0_p\rangle(|1_{\mathrm{TE}\nu}\rangle|0_{\mathrm{TM}\nu}\rangle|0_{\mathrm{TE}(-\nu)}\rangle|1_{\mathrm{TM}(-\nu)}\rangle + e^{i\varphi_z}|0_{\mathrm{TE}\nu}\rangle|1_{\mathrm{TM}\nu}\rangle|1_{\mathrm{TE}(-\nu)}\rangle|0_{\mathrm{TM}(-\nu)}\rangle),\end{aligned} \tag{B17}$$

where

$$\varphi_z = \mathrm{Arg}\left[\frac{\sin K_R z + i\frac{\delta}{K_R}(\cos K_R z - 1)}{\sin K_R z - i\frac{\delta}{K_R}(\cos K_R z - 1)}\right]. \tag{B18}$$

Equation (B17) is the generalization of a tripartite entangled state of the GHZ type [45,49–52] to the case when the selection rules and conservation laws allow the decay of an initial excitation of the system into any of the two "allowed" boson pairs.

For small group velocity mismatch, when $\nu|\frac{1}{\upsilon_{\mathrm{TM}}} - \frac{1}{\upsilon_{\mathrm{TE}}}| \ll \frac{\sqrt{2Q_0}|G|}{\hbar} \approx K_R$, the quantum state in the waveguide cross sections defined by $K_R z = \frac{\pi}{2} + \pi M$,

$$|\Psi\rangle \approx |0_p\rangle\frac{|1_{\mathrm{TE}\nu}\rangle|0_{\mathrm{TM}\nu}\rangle|0_{\mathrm{TE}(-\nu)}\rangle|1_{\mathrm{TM}(-\nu)}\rangle + |0_{\mathrm{TE}\nu}\rangle|1_{\mathrm{TM}\nu}\rangle|1_{\mathrm{TE}(-\nu)}\rangle|0_{\mathrm{TM}(-\nu)}\rangle}{\sqrt{2}}, \tag{B19}$$

is one of the entangled Bell states.

Here we considered the parametric decay into two relatively narrow spectral bands. Now consider a broadband decay in which the total width of the SPDC spectrum is $\Delta\Omega \gg \Delta\omega$. We will use the method developed in [54] for strong coupling in the systems with inhomogeneous broadening of the spectra.

The solution to Eq. (B6) for the initial conditions $C_{W\nu} = 0$ is

$$C_{W\nu} = -iG\sqrt{\frac{\Delta\omega}{2\pi}}\int_0^z e^{i\delta_\nu(z-\xi)}C_p(\xi)d\xi. \tag{B20}$$

Substituting it into Eq. (B5) gives

$$\frac{\partial}{\partial z}C_p = -|G|^2\frac{\Delta\omega}{2\pi}\sum_{\nu}\int_0^z e^{i\delta_\nu(z-\xi)}C_p(\xi)d\xi. \tag{B21}$$

Since the spectrum of decay photons is split into the bands of width $\Delta\omega$, we can transform Eq. (B21) as

$$\frac{\partial}{\partial z}C_p = -|G|^2\frac{\Delta\omega}{2\pi}\sum_{m=-M}^{m=M}\int_0^z e^{i\delta_m(z-\xi)}C_p(\xi)d\xi, \tag{B22}$$

where

$$\delta_m = m\Delta\omega\left(\frac{1}{v_{\rm TM}} - \frac{1}{v_{\rm TE}}\right) \tag{B23}$$

and $M = [\frac{\Delta\Omega}{2\Delta\omega}]$. Going from summation to integration in Eq. (B22),

$$\sum_{m=-M}^{m=M} \int_0^z e^{i\delta_m(z-\xi)} C_p(\xi) d\xi$$
$$\Rightarrow \int_{-\Gamma/2}^{\Gamma/2} \frac{d\delta}{\Delta\omega\left|\frac{1}{v_{\rm TM}} - \frac{1}{v_{\rm TE}}\right|} \int_0^z e^{i\delta(z-\xi)} C_p(\xi) d\xi, \tag{B24}$$

where

$$\Gamma = \Delta\Omega\left|\frac{1}{v_{\rm TM}} - \frac{1}{v_{\rm TE}}\right|, \tag{B25}$$

we arrive at

$$\frac{\partial}{\partial z} C_p = -\frac{|G|^2}{\left|\frac{1}{v_{\rm TM}} - \frac{1}{v_{\rm TE}}\right|} \int_0^z d\xi \left[\frac{\sin\left[\frac{\Gamma}{2}(z-\xi)\right]}{\pi(z-\xi)}\right] C_p(\xi). \tag{B26}$$

Let us denote by λ a typical spatial scale of the function $C_p(\xi)$. If $\frac{\Gamma}{2}\lambda \gg 1$, one can replace $\frac{\sin[\frac{\Gamma}{2}(z-\xi)]}{\pi(z-\xi)} \Rightarrow \delta(z-\xi)$ in Eq. (B26), which gives

$$\frac{\partial}{\partial z} C_p = -\kappa C_p, \tag{B27}$$

where

$$\kappa = \frac{|G|^2}{\left|\frac{1}{v_{\rm TM}} - \frac{1}{v_{\rm TE}}\right|}. \tag{B28}$$

For the initial condition $C_p = 1$ we obtain

$$C_p = e^{-\kappa z}. \tag{B29}$$

Equations (B27) and (B29) are valid when $\frac{\Gamma}{2\kappa} \gg 1$, which corresponds to the condition

$$\alpha = \frac{\sqrt{\Delta\Omega}}{|G|}\left|\frac{1}{v_{\rm TM}} - \frac{1}{v_{\rm TE}}\right| \gg 1. \tag{B30}$$

In the opposite limit $\frac{\Gamma}{2}\lambda \ll 1$ we will seek the solution of Eq. (B26) as $C_p \propto e^{qz}$. The right-hand side of Eq. (B26) can be expanded in powers of q^{-1} by repeated integration by parts. Denoting $\frac{\sin[\frac{\Gamma}{2}(\xi-z)]}{\pi(\xi-z)} = D(\xi - z)$ and taking into account $\Gamma z \gg 1$, we obtain

$$\int_{-\infty}^z d\xi D(\xi - z) e^{q\xi}$$
$$= \left(\frac{D(0)}{q} + \sum_{n=1}^{\infty} (-1)^n \left[\frac{d^n D(\xi - z)}{d\xi^n}\right]_{\xi=z} \frac{1}{q^{n+1}}\right) e^{qz},$$

where

$$\left[\frac{d^{2n+1} D(\xi - z)}{d\xi^{2n+1}}\right]_{\xi=z} = 0,$$
$$\left[\frac{d^{2n} D(\xi - z)}{d\xi^{2n}}\right]_{\xi=z} = \frac{(-1)^n \left(\frac{\Gamma}{2}\right)^{2n+1}}{\pi(2n+1)}.$$

Taking into account that $\frac{|G|^2}{\left|\frac{1}{v_{\rm TM}} - \frac{1}{v_{\rm TE}}\right|} \frac{\Gamma}{2\pi} = |G|^2 \frac{\Delta\Omega}{2\pi}$, we obtain from Eq. (B26) that

$$q^2 + |G|^2 \frac{\Delta\Omega}{2\pi}\left[1 - \sum_{n=1}^{\infty} \frac{(-1)^n}{2n+1}\left(\frac{\Gamma}{2q}\right)^{2n}\right] = 0. \tag{B31}$$

In zeroth order with respect to a small parameter $\frac{\Gamma}{2q}$ we have

$$q^2 + |G|^2 \frac{\Delta\Omega}{2\pi} = 0;\ C_p \propto e^{\pm i|G|\sqrt{\frac{\Delta\Omega}{2\pi}} z}. \tag{B32}$$

For the initial condition $C_p = 1$ this solution corresponds to spatial Rabi oscillations:

$$C_p \approx \cos\left(|G|\sqrt{\frac{\Delta\Omega}{2\pi}} z\right). \tag{B33}$$

Equation (B33) is valid when $\frac{\Gamma}{2|G|\sqrt{\frac{\Delta\Omega}{2\pi}}} \ll 1$, which corresponds to the region of parameters opposite to that of Eq. (B30), i.e., $\alpha \ll 1$.

Let us now discuss the corrections due to higher-order terms with respect to a small parameter $\frac{\Gamma}{2q}$. Substituting $q = q_0 + \eta$ into Eq. (B31), where $q_0 = \pm i|G|\sqrt{\frac{\Delta\Omega}{2\pi}}$ and $|q_0| \gg |\eta|$, we obtain

$$\eta = \frac{|G|^2 \frac{\Delta\Omega}{2\pi} \sum_{n=1}^{\infty} \frac{(-1)^n}{2n+1}\left(\frac{\Gamma}{2q_0}\right)^{2n}}{2q_0 + \frac{|G|^2 \frac{\Delta\Omega}{2\pi}}{q_0} \sum_{n=1}^{\infty} \frac{(-1)^n 2n}{2n+1}\left(\frac{\Gamma}{2q_0}\right)^{2n}}. \tag{B34}$$

It is easy to see that all terms in the numerator of Eq. (B34) are real whereas all terms in the denominator are imaginary. Therefore, η is imaginary, i.e., it changes the wave number but not the decay constant. This is true in any order with respect to $\frac{\Gamma}{2|q_0|}$.

The amplitudes C_{Wv} are easily calculated by substituting the expression for C_p from Eq. (B29) or Eq. (B33) into Eq. (B20).

[1] J. P. Torres, K. Banaszek, and I. A. Walmsley, Engineering Nonlinear Optic Sources of Photonic Entanglement, Prog. Opt. **56**, 227 (2011).

[2] C. Couteau, Spontaneous parametric down-conversion, Contemp. Phys. **59**, 291 (2018).

[3] P. G. Kwiat, K. Mattle, H. Weinfurter, A. Zeilinger, A. V. Sergienko, and Y. Shih, New High-Intensity Source of Polarization-Entangled Photon Pairs, Phys. Rev. Lett. **75**, 4337 (1995).

[4] M. Lapine, I. V. Shadrivov, and Y. S. Kivshar, Colloquium: Nonlinear metamaterials, Rev. Mod. Phys. **86**, 1093 (2014).

[5] D. Smirnova and Y. S. Kivshar, Multipolar nonlinear nanophotonics, Optica **3**, 1241 (2016).

[6] A. R. Davoyan and H. A. Atwater, Quantum nonlinear light emission in metamaterials: broadband Purcell enhancement of parametric downconversion, Optica **5**, 608 (2018).

[7] J. U. Furst, D. V. Strekalov, D. Elser, A. Aiello, U. L. Andersen, Ch. Marquardt, and G. Leuchs, Low-Threshold Optical Parametric Oscillations in a Whispering Gallery Mode Resonator, Phys. Rev. Lett. **105**, 263904 (2010).

[8] A. S. Solntsev and A. A. Sukhorukov, Path-entangled photon sources on nonlinear chips, Rev. Phys. **2**, 19 (2017).

[9] G. Marino, A. S. Solntsev, L. Xu, V. F. Gili, L. Carletti, A. N. Poddubny, M. Rahmani, D. A. Smirnova, H. Chen, A. Lemaitre, G. Zhang, A. V. Zayats, C. De Angelis, G. Leo, A. A. Sukhorukov, and D. N. Neshev, Spontaneous photon-pair generation from a dielectric nanoantenna, Optica **6**, 1416 (2019).

[10] Z. Ma, J. Chen, Z. Li, C. Tang, Y. Sua, H. Fan, and Y. Huang, Ultrabright Quantum Photon Sources on Chip, Phys. Rev. Lett. **125**, 263602 (2020).

[11] J. Wang, F. Sciarrino, A. Laing, and M. G. Thompson, Integrated photonic quantum technologies, Nat. Photonics **14**, 273 (2020).

[12] R. Horn, P. Abolghasem, B. J. Bijlani, D. Kang, A. S. Helmy, and G. Weihs, Monolithic Source of Photon Pairs, Phys. Rev. Lett. **108**, 153605 (2012).

[13] D. Kang, A. Anirban, and A. S. Helmy, Monolithic semiconductor chips as a source for broadband wavelength-multiplexed polarization entangled photons, Opt. Express **24**, 15160 (2016).

[14] J. Svozilik, M. Hendrych, and J. P. Torres, Bragg reflection waveguide as a source of wavelength-multiplexed polarization-entangled photon pairs, Opt. Express **20**, 15015 (2012).

[15] B. J. Bijlani, P. Abolghasem, and A. S. Helmy, Semiconductor optical parametric generators in isotropic semiconductor diode lasers, Appl. Phys. Lett. **103**, 091103 (2013).

[16] F. Boitier, A. Orieux, C. Autebert, A. Lemaître, E. Galopin, C. Manquest, C. Sirtori, I. Favero, G. Leo, and S. Ducci, Electrically Injected Photon-Pair Source at Room Temperature, Phys. Rev. Lett. **112**, 183901 (2014).

[17] I. Shoji, T. Kondo, A. Kitamoto, M. Shirane, and R. Ito, Absolute scale of second-order nonlinear-optical coefficients, J. Opt. Soc. Am. B **14**, 2268 (1997).

[18] G. W. Gardiner and C. M. Savage, A multimode quantum theory of a degenerate parametric amplifier in a cavity, Opt. Commun. **50**, 173 (1984).

[19] H. J. Carmichael, *Statistical Methods in Quantum Optics* (Springer-Verlag, Berlin, 2008), Vol. 2, Chap. 9.

[20] M. O. Scully and M. S. Zubairy, *Quantum Optics* (Cambridge University, Cambridge, England, 1997).

[21] M. D. Reid and D. F. Walls, Generation of squeezed states via degenerate four-wave mixing, Phys. Rev. A **31**, 1622 (1985).

[22] P. Kolchin, Electromagnetically-induced-transparency-based paired photon generation, Phys. Rev. A **75**, 033814 (2007).

[23] V. Vdovin and M. Tokman, Generation of a two-mode squeezed vacuum field in forward four-wave mixing process in an ensemble of Lambda atoms, Phys. Rev. A **87**, 012323 (2013).

[24] M. Erukhimova and M. Tokman, Squeezing of thermal fluctuations in four-wave mixing in a Λ-scheme, Phys. Rev. A **95**, 013807 (2017).

[25] S.-K. Liao, W.-Q. Cai, J. Handsteiner, B. Liu, J. Yin, L. Zhang, D. Rauch, M. Fink, J.-G. Ren, W.-Y. Liu, Y. Li, Q. Shen, Y. Cao, F.-Z. Li, J.-F. Wang, Y.-M. Huang, L. Deng, T. Xi, L. Ma, T. Hu, L. Li, N.-L. Liu, F. Koidl, P. Wang, Y.-A. Chen, X.-B. Wang, M. Steindorfer, G. Kirchner, C.-Y. Lu, R. Shu, R. Ursin, T. Scheidl, C.-Z. Peng, J.-Y. Wang, A. Zeilinger, and J.-W. Pan, Satellite-Relayed Intercontinental Quantum Network, Phys. Rev. Lett. **120**, 030501 (2018).

[26] S.-K. Liao, H.-L. Yong, C. Liu, G.-L. Shentu, D.-D. Li, J. Lin, H. Dai, S.-Q. Zhao, B. Li, J.-Y. Guan *et al.*, Long-distance free-space quantum key distribution in daylight towards inter-satellite communication, Nat. Photonics **11**, 509 (2017).

[27] ASTM E490-00a(2019), Standard Solar Constant and Zero Air Mass Solar Spectral Irradiance Tables (American Society for Testing and Materials, Washington, DC, 2019).

[28] H. Kaushal and G. Kaddoum, Optical communication in space: Challenges and mitigation techniques, IEEE Commun. Surv. Tutorials **19**, 57 (2017).

[29] T. Gregory, P.-A. Moreau, E. Toninelli, and M. J. Padgett, Imaging through noise with quantum illumination, Sci. Adv. **6**, eaay2652 (2020).

[30] S. Prabhakar, T. Shields, A. C. Dada, M. Ebrahim, G. G. Taylor, D. Morozov, K. Erotokritou, S. Miki, M. Yabuno, H. Terai, C. Gawith, M. Kues, L. Caspani, R. H. Hadfield, and M. Clerici, Two-photon quantum interference and entanglement at 2.1 μm, Sci. Adv. **6**, eaay5195 (2020).

[31] R. A. McCracken, F. Grafitti, and A. Fedrizzi, Numerical investigation of mid-infrared single-photon generation, J. Opt. Soc. Am. B **35**, C38 (2018).

[32] M. Mancinelli, A. Trenti, S. Piccione, G. Fontana, J. S. Dam, P. Tidemand-Lichtenberg, C. Pedersen, and L. Pavesi, Mid-infrared coincidence measurements on twin photons at room temperature, Nat. Commun. **8**, 15184 (2017).

[33] M. Tokman, Z. Long, S. Al Mutairi, Y. Wang, V. Vdovin, M. Belkin, and A. Belyanin, Purcell enhancement of the parametric down-conversion in two-dimensional nonlinear materials, APL Photonics **4**, 034403 (2019).

[34] V. M. Fain and Y. I. Khanin, *Quantum Electronics: Basic Theory* (MIT, Cambridge, MA, 1969).

[35] M. D. Tokman, M. A. Erukhimova, and V. V. Vdovin, The features of a quantum description of radiation in an optically dense medium, Ann. Phys. (NY) **360**, 571 (2015).

[36] V. L. Ginzburg and V. M. Agranovich, *Spatial Dispersion in Crystal Optics and the Theory of Excitons* (Wiley, New York, 1966).

[37] M. H. Rubin, D. N. Klyshko, Y. H. Shih, and A. V. Sergienko, Theory of two-photon entanglement in type-II optical parametric down-conversion, Phys. Rev. A **50**, 5122 (1994).

[38] Y. A. Il'inskii and L. V. Keldysh, *Electromagnetic Response of Material Media* (Springer, New York, 1994).

[39] M. Tokman, Y. Wang, and A. Belyanin, Valley entanglement of excitons in monolayers of transition-metal dichalcogenides, Phys. Rev. B **92**, 075409 (2015).

[40] M. Tokman, X. Yao, and A. Belyanin, Generation of Entangled Photons in Graphene in a Strong Magnetic Field, Phys. Rev. Lett. **110**, 077404 (2013).

[41] N. Sisakyan and Yu. Malakyan, Creation of a photonic time-bin qubit via parametric interaction of photons in a driven resonant medium, Phys. Rev. A **75**, 063831 (2007).

[42] M. Tokman, Y. Wang, I. Oladyshkin, A. R. Kutayiah, and A. Belyanin, Laser-driven parametric instability and generation of entangled photon-plasmon states in graphene and topological insulators, Phys. Rev. B **93**, 235422 (2016).

[43] M. Tokman, Z. Long, S. Al Mutairi, Y. Wang, M. Belkin, and A. Belyanin, Enhancement of the spontaneous emission in subwavelength quasi-two-dimensional waveguides and resonators, Phys. Rev. A **97**, 043801 (2018).

[44] D. A. Antonosyan, A. S. Solntsev, and A. A. Sukhorukov, Single-photon spontaneous parametric down-conversion in quadratic nonlinear waveguide arrays, Opt. Commun. **327**, 22 (2014).

[45] M. Tokman, M. Erukhimova, Y. Wang, Q. Chen, and A. Belyanin, Generation and dynamics of entangled fermion-photon-phonon states in nanocavities, Nanophotonics **10**, 491 (2021).

[46] Q. Chen, Y. Wang, S. Almutairi, M. Erukhimova, M. Tokman, and A. Belyanin, Dynamics and control of entangled electron-photon states in nanophotonic systems with time-variable parameters, Phys. Rev. A **103**, 013708 (2021).

[47] M. B. Plenio and P. L. Knight, The quantum-jump approach to dissipative dynamics in quantum optics, Rev. Mod. Phys. **70**, 101 (1998).

[48] L. Mandel and E. Wolf, *Optical Coherence and Quantum Optics* (Cambridge University, Cambridge, England, 2013).

[49] W. Dur, G. Vidal, and J. I. Cirac, Three qubits can be entangled in two inequivalent ways, Phys. Rev. A **62**, 062314 (2000).

[50] M. M. Cunha, A. Fonseca, and E. O. Silva, Tripartite entanglement: Foundations and applications, Universe **5**, 209 (2019).

[51] L. K. Shalm, D. R. Hamel, Z. Yan, C. Simon, K. J. Resch, and T. Jennewein, Three-photon energy-time entanglement, Nat. Phys. **9**, 19 (2013).

[52] A. Agusti, C. W. Sandbo Chang, F. Quijandria, G. Johansson, C. M. Wilson, and C. Sabin, Tripartite Genuine Non-Gaussian Entanglement in Three-Mode Spontaneous Parametric Down-Conversion, Phys. Rev. Lett. **125**, 020502 (2020).

[53] N. K. Langford, S. Ramelow, R. Prevedel, W. J. Munro, J. Milburn, and A. Zeilinger, Efficient quantum computing using coherent photon conversion, Nature (London) **478**, 360 (2011).

[54] M. Tokman, Q. Chen, M. Erukhimova, Y. Wang, and A. Belyanin, Quantum dynamics of open many-qubit systems strongly coupled to a quantized electromagnetic field in dissipative cavities, arXiv:2105.14674 v1.

[55] N. Bloembergen, *Nonlinear Optics* (World Scientific, Singapore, 1996).

[56] G. A. Korn and T. M. Korn, *Mathematical Handbook for Scientists and Engineers* (McGraw-Hill, New York, 1968).